Molecular Biology of the Cell
Vol. 20, 3224–3238, July 15, 2009

Filamin A–β1 Integrin Complex Tunes Epithelial Cell Response to Matrix Tension

Scott Gehler,[*†] Massimiliano Baldassarre,[‡] Yatish Lad,[‡] Jennifer L. Leight,[§‖] Michele A. Wozniak,[*§] Kristin M. Riching,[*†] Kevin W. Eliceiri,[†] Valerie M. Weaver,[‖] David A. Calderwood,[‡] and Patricia J. Keely[*†]

[*]Department of Pharmacology and [†]Laboratory for Optical and Computational Instrumentation, University of Wisconsin, Madison, WI 53706; [‡]Department of Pharmacology and Interdepartmental Program in Vascular Biology and Transplantation, Yale University School of Medicine, New Haven, CT 06520; [§]Department of Bioengineering, University of Pennsylvania, Philadelphia, PA 19104; and [‖]Center for Bioengineering and Tissue Regeneration, Department of Surgery, University of California, San Francisco, CA 94143

Submitted December 11, 2008; Revised April 22, 2009; Accepted May 13, 2009
Monitoring Editor: Yu-Li Wang

The physical properties of the extracellular matrix (ECM) regulate the behavior of several cell types; yet, mechanisms by which cells recognize and respond to changes in these properties are not clear. For example, breast epithelial cells undergo ductal morphogenesis only when cultured in a compliant collagen matrix, but not when the tension of the matrix is increased by loading collagen gels or by increasing collagen density. We report that the actin-binding protein filamin A (FLNa) is necessary for cells to contract collagen gels, and pull on collagen fibrils, which leads to collagen remodeling and morphogenesis in compliant, low-density gels. In stiffer, high-density gels, cells are not able to contract and remodel the matrix, and morphogenesis does not occur. However, increased FLNa-β1 integrin interactions rescue gel contraction and remodeling in high-density gels, resulting in branching morphogenesis. These results suggest morphogenesis can be "tuned" by the balance between cell-generated contractility and opposing matrix stiffness. Our findings support a role for FLNa-β1 integrin as a mechanosensitive complex that bidirectionally senses the tension of the matrix and, in turn, regulates cellular contractility and response to this matrix tension.

INTRODUCTION

The compliance of the extracellular matrix (ECM) and cellular regulation of matrix remodeling are critical determinants of tissue morphogenesis, tumor invasion, and wound healing (Larsen *et al*., 2006). Increasing the matrix tension by culturing cells in a stiff or a loaded three-dimensional (3D) matrix perturbs morphogenesis of fibroblasts and breast epithelial cells (Wozniak *et al*., 2003; Paszek *et al*., 2005; Guo *et al*., 2006). Cells exert mechanical force on the ECM, which results in matrix remodeling and collagen fibril translocation (Miron-Mendoza *et al*., 2008) and myosin-mediated contractility (Discher *et al*., 2005; Giannone and Sheetz, 2006). Along these lines, inhibition of myosin activity disrupts cell morphogenesis and collagen matrix organization (Wozniak *et al*., 2003; Meshel *et al*., 2005; Paszek *et al*., 2005; Guo *et al*., 2006). Consequently, cells are able to "feel" the stiffness of their microenvironment and respond through mechanical feedback to regulate cell contractility and cell behavior. Although the interplay between matrix stiffness and cell contractility is essential for morphogenesis, the signaling mechanisms by which cells detect mechanical cues and transduce this information into biochemical signals is not well understood.

Because integrins link the ECM to the cytoskeleton through scaffolding proteins, integrins and focal adhesions have been proposed to play an integral role in mechanotransduction. Cells respond to mechanical cues by strengthening integrin–cytoskeletal attachments (Choquet *et al*., 1997; Pelham and Wang, 1997). Furthermore, changes in ECM stiffness or internal force generation alter integrin–cytoskeletal connections to induce changes in cell morphogenesis and matrix remodeling (Giannone and Sheetz, 2006). For example, inhibition of α2β1 integrin function affects collagen matrix contraction and organization and disrupts cell morphology (Schiro *et al*., 1991). Although it is apparent that cells encountering matrices of different physical properties alter their integrin–cytoskeletal linkages, it is not clear mechanistically how this occurs.

The actin-binding protein filamin A (FLNa) interacts with the cytoplasmic domain of β1 integrin to regulate integrin function (Loo *et al*., 1998; Pfaff *et al*., 1998; Calderwood *et al*., 2001). Not only does FLNa scaffold several signaling molecules but also it is postulated to act as a mechanosensor in cells (Stossel *et al*., 2001). In support of this, FLNa accumulates at adhesion sites in response to mechanical tension and is important for tension-induced actin accumulation at these sites (Glogauer *et al*., 1998; D'Addario *et al*., 2002). Moreover, FLNa cross-links the actin cytoskeleton and regulates the tension of polymerized actin networks (DiDonna and Levine, 2006; Gardel *et al*., 2006). FLNa can potentiate actomy-

This article was published online ahead of print in *MBC in Press* (http://www.molbiolcell.org/cgi/doi/10.1091/mbc.E08–12–1186) on May 20, 2009.

Address correspondence to: Patricia J. Keely (pjkeely@wisc.edu).

Abbreviations used: FILIP, filamin A-interacting protein; FLNa, filamin A; MLC, myosin light chain; MPLSM, multiphoton laser-scanning microscopy; SHG, second-harmonic generation.

osin ATPase activity in vitro (Sosinski *et al*., 1984; Janson *et al*., 1991) and bind regulators of myosin-mediated contractility (Ohta *et al*., 1999; Pi *et al*., 2002; Ueda *et al*., 2003). Therefore, we hypothesize that FLNa-β1 integrin complexes could serve as a mechanical or biochemical link that couples the actin cytoskeleton to the ECM and regulate cell morphogenesis in response to the stiffness of the extracellular matrix.

High breast density is linked to an increased risk of breast carcinoma (Boyd *et al*., 2001), and it is associated with a significant increase in the deposition of extracellular matrix components, especially collagen and fibronectin (Guo *et al*., 2001). It has been demonstrated that the stiffness of a collagen matrix increases with increasing collagen concentration (Roeder *et al*., 2002; Paszek *et al*., 2005). Thus, understanding how cells respond to matrix stiffness could inform an understanding of how breast density links to carcinoma risk. Using 3D collagen gels, we show that FLNa binding to β1 integrin is essential for cells to contract and remodel collagen matrices, and this is in turn essential for ductal morphogenesis. Furthermore, enhanced FLNa-β1 integrin interactions are sufficient to "tune" branching morphogenesis in stiffer, high-density gels. Our results suggest FLNa-β1 integrin complexes serve as part of the mechanosensitive machinery that both senses matrix tension and regulates collagen matrix contraction and cell morphogenesis in response to the physical properties of the matrix.

MATERIALS AND METHODS

Reagents

Collagen type I was obtained from BD Biosciences Discovery (Bedford, MA). Antibodies used include the following: human (h)FLNa and β1 integrin (Millipore, Billerica, MA), anti-human β1 integrin 12G10, mouse (m)FLNa (Cell Signaling Technology, Beverly, MA), rabbit glyceraldehyde-3-phosphate dehydrogenase (GAPDH) (Santa Cruz Biotechnology, Santa Cruz, CA), rabbit green fluorescent protein (GFP) (Sigma-Aldrich, St. Louis, MO), and phosphomyosin light chain (MLC) antibodies (Ser19 and Thr18/Ser19) and total MLC (Cell Signaling Technology). Bisbenzimide was purchased from Sigma-Aldrich, and AlexaFluor594 phalloidin was obtained from Invitrogen (Carlsbad, CA). Horseradish peroxidase (HRP)-conjugated secondary antibodies were from Jackson ImmunoResearch Laboratories (West Grove, PA). Blebbistatin was obtained from Calbiochem (San Diego, CA). All culture media were purchased from Invitrogen.

Cell Culture and Transfection

T47D cells were obtained from American Type Culture Collection (Manassas, VA) and maintained as described previously (Keely *et al*., 1995). Normal murine mammary gland (NMuMG) cells were kindly provided by Dr. Caroline Alexander (University of Wisconsin, Madison, WI) and maintained in DMEM containing 10% fetal bovine serum. Cells were stably transfected with hFLNa short hairpin RNA (shRNA), filamin A interacting protein (FILIP) shRNA, or luciferase shRNA control vectors (Open Biosystems, Huntsville, AL), GFP-IgFLNa21 or GFP-IgFLNa21(I/C) control (Kiema *et al*., 2006), and hβ1 or hβ1(V787,791I) (Calderwood *et al*., 2001). For FLNa-GFP, FLNa was subcloned into pCDNA3. An in-frame GFP, generated by polymerase chain reaction (PCR), was subcloned directly C-terminal to IgFLNa24 (Lad *et al*., 2007). Cells expressing GFP-tagged constructs were sorted for equal expression. NMuMG cells expressing hβ1 or hβ1(V787,791I) were sorted via indirect immunofluorescence using a β1 antibody that recognizes only human β1 integrin.

Cells were cultured in collagen type I gels as described previously (Keely *et al*., 1995). Gels containing T47D or NMuMG cells were poured into six-well plates and allowed to polymerize for 4 h at 37°C. Two milliliters of complete media was added, and gels were either detached from the sides of the dish (floating) or left attached. The time at which the gels were rendered floating was considered day 0. For myosin inhibitor experiments, 20 μM blebbistatin was added at the time the gels were released. Gel media (containing blebbistatin, if applicable) was replenished every 4 d, and morphogenesis was assessed after 10 d in culture. Phase contrast microscopy was carried out using a Nikon TE300 inverted microscope equipped with a CoolSNAP fx charge-coupled device (CCD) camera (Photometrics, Tucson, AZ). Images were acquired using SlideBook, version 4.2 (Intelligent Imaging Innovations, Denver, CO) and processed using Adobe Photoshop CS2 (Adobe Systems, San Jose, CA).

Elastic Modulus Measurements

Collagen-I HC (high concentration BD) samples were tested on a controlled strain rheometer (RFS-III; Rheometric Scientific, Piscataway, NJ) at 37°C, 2% strain, and a frequency of 10 rad/s. Samples were preformed in a plastic washer (d = 8.5 mm, t = 1.45 mm) (McMaster-Carr, Cleveland, OH), polymerized at 37°C for 45 min, and tested with an 8-mm parallel plate geometry. Elastic modulus was calculated from shear modulus measurements (Poisson's ratio = 0.5).

Collagen Matrix Contraction Measurements

Gel contraction measurements were performed as described previously (Keely *et al*., 2007). Gels were poured and released as described above. The time at which the gels were rendered floating was considered day 0. Gel diameter was measured every day for 10 d and was presented as total contraction (in millimeters) over time or as contraction at day 10 (T47Ds) or day 4 (NMuMGs).

Second harmonic generation and multiphoton microscopy was performed on collagen gels that were fixed with 2% paraformaldehyde for 15 min before imaging. All images were acquired using a custom-designed multiphoton laser-scanning optical workstation (Wokosin *et al*., 2003). Gels were imaged using a TE300 inverted microscope (Nikon, Tokyo, Japan) equipped with a 40× Plan Fluor oil immersion objective (numerical aperture 1.3; Nikon) by using a mode-locked Ti:sapphire laser (Spectra Physics Millennium/Tsunami, Mountain View, CA) with excitation wavelength tuned at 890 nm. A 445 nm narrow band pass filter (Thin Film Imaging, Greenfield, MA) was used to detect the second-harmonic generation (SHG) signal of collagen, whereas a 520/35 nm filter (Semrock, Rochester, NY) was used to detect cell autofluorescence or GFP signal. Serial image planes were acquired at 1-μm steps in z depth surrounding cell structures. Image acquisition was performed using WiscScan (http://www.loci.wisc.edu/wiscscan/). Images were analyzed using ImageJ, version 1.39o (National Institutes of Health, Bethesda, MD) and processed using Photoshop CS2.

Fluorescence intensity of collagen fibrils was measured along a 1-pixel-wide, 50-μm-long line that was drawn from the edge of the cell–ECM boundary (0 μm) into the collagen matrix. Measurements were taken from multiple regions from each gel. Regions where cell structures were within 100 μm of each other were not included in the measurements. Intensity measurements were averaged and graphed over distance from the cell–ECM boundary (0 μm). All measurements were acquired and analyzed using ImageJ, version 1.39o. Statistical analysis was performed by comparing the intensity value on the line scan at 5 μm out from the cell boundary for each sample, averaging three imaging fields from duplicates or triplicates for each experiment. Each experiment was repeated three times. Two-tailed *t* tests were then performed between samples from a single experiment where imaging was performed on the same day and conditions were matched for intensity comparisons. As a second approach, regression analysis and one-way analysis of variance was performed for all experiments, and further confirmed statistical significance.

Myosin Activity Assay

Phosphorylated (p)MLC levels were used to assess the amount of myosin activity of cells in collagen gels. Cells were detached using 0.5 mM EDTA in phosphate-buffered saline (PBS) and were resuspended in serum-free media plus 5 mg/ml bovine serum albumin (BSA) to eliminate the effects of serum stimulation. Gels (400 μl) containing 2 million cells were poured in 12-well plates and allowed to incubate 1 h at 37°C. Gels were released and incubated an additional 90 min. Cells in gels were lysed using an equal volume of 2× sample buffer [125 mM Tris-HCl, pH 6.8, 4% SDS, 20% glycerol, 100 mM dithiothreitol, and 0.02% bromphenol blue] followed by heating the sample for 15 min at 95°C. Samples were separated using SDS-polyacrylamide gel electrophoresis (PAGE) and transferred onto polyvinylidene difluoride (PVDF) membranes. Membranes were blocked with 5% nonfat milk plus 0.1% Tween 20 in Tris-buffered saline (TBS) for 1 h at room temperature and then incubated with 1:1000 pMLC(Ser19) or pMLC(Thr18/Ser19) overnight at 4°C. After rinsing, membranes were incubated with a HRP-conjugated rabbit secondary and then visualized using enhanced chemiluminescence (ECL) reagents (GE Healthcare, Chalfont St. Giles, Buckinghamshire, United Kingdom). Membranes were reprobed using 1:500 total MLC. pMLC was normalized to total MLC by densitometry using ImageJ.

Western Blotting and Immunoprecipitations

Protein expression was assessed through immunoblotting. In brief, cells were lysed in denaturing Laemmli buffer followed by protein separation using SDS-PAGE. After proteins were transferred onto PVDF membrane, membranes were blocked using 5% milk plus 0.3% Tween 20 in TBS. Membranes were probed with either 1:1000 anti-hFLNa, 1:1000 anti-mFLNa, or 1:2000 anti-GAPDH, followed by incubation with 1:5000 HRP-conjugated secondary antibodies. Membranes were visualized using ECL reagents (GE Healthcare).

Immunoprecipitations of β1 integrin were performed as described previously (Keely *et al*., 2007). Briefly, gels containing 10 million cells were made with BSA in RPMI 1640 medium or DMEM. After gels were allowed to polymerize for 1 h, gels were released as described above. Gels incubated for

an additional 1 h at 37°C. Cells in gels were lysed with 2× lysis buffer (50 mM HEPES, pH 7.4, 100 mM NaCl, 10 mM EDTA, 0.2% BSA, 0.2% Triton X-100, 10 mM NaF, 1 mM pervanadate, and protease inhibitors) and incubated at 4°C for 20 min. After centrifugation, supernatants were incubated with β1 integrin antibody plus 30 μl of GammaBind G-Sepharose (GE Healthcare) overnight at 4°C. Samples were washed extensively with lysis buffer followed by denaturation with Laemmli buffer. Samples were separated using SDS-PAGE and transferred onto PVDF membranes. Membranes were blocked with 3% BSA plus 0.3% Tween 20 in TBS and then incubated with FLNa or β1 integrin antibodies. After incubation with secondary antibodies, membranes were rinsed and then visualized using ECL reagents (GE Healthcare). FLNa was normalized to β1 integrin by densitometry using ImageJ. All digital images for micrographs and blots were processed and produced using Adobe Photoshop CS2 (Adobe Systems).

Immunofluorescence

Immunofluorescence in 3D collagen gels was carried out as described previously (Wozniak *et al*., 2003). Briefly, T47D cells were cultured in collagen gels for 10 d. Gels were fixed with 4% paraformaldehyde and labeled with 1:2000 AlexaFluor594 phalloidin (Invitrogen) and 1:2000 bisbenzimide (Sigma-Aldrich). Fluorescence microscopy was carried out using a Nikon TE300 inverted microscope equipped with a CoolSNAP fx CCD camera (Photometrics). Images were acquired using SlideBook, version 4.2 (Intelligent Imaging Innovations) and processed using Adobe Photoshop CS2 (Adobe Systems).

RESULTS

Increased Collagen Density and Stiffness Disrupts Collagen Matrix Contraction and Ductal Morphogenesis

We previously showed that the density of a collagen gel, which can be altered by increasing the collagen concentration, regulates breast epithelial cell morphogenesis (Wozniak *et al*., 2003). Well-differentiated human T47D breast carcinoma cells underwent ductal morphogenesis only when cultured in low-density (1.0 mg/ml), floating collagen gels (Figure 1Aa). If these same gels were left attached to the dish, such that the gel cannot be contracted, then morphogenesis was disrupted (Figure 1Bb). Because attached gels are typically thought of as mechanically loaded because cellular contraction on the gel is met with resistance, the failure of cells to form tubules in an otherwise identical collagen matrix demonstrates that these cells must be in a compliant matrix to undergo this type of morphogenesis. In this case, tubulogenesis is defined by the formation of thin, hollow tubes composed of one cell layer and a lumen (Keely *et al*., 1995). Similar to cells in mechanically loaded gels, cells cultured in high-density (2.0 mg/ml) floating gels also fail to undergo tubulogenesis (Figure 1, C and D, c and d). This likely reflects an increased stiffness in high-density gels, because the elastic modulus increased with increasing collagen concentration (Figure 1E). This finding is consistent with the results of others, in which increased collagen gel concentrations result in an increased modulus, as measured using both compression or tensile testing (Roeder *et al*., 2002; Paszek *et al*., 2005). It is likely that the response of cells to the high-density (2.0 mg/ml) gel is due to the effect of matrix stiffness rather than due to increased ligand concentration, because cells in the attached low-density (1.0 mg/ml) gel phenocopy the high-density gel (compare Figure 1B with C). Thus, increased matrix stiffness, whether due to constraint, or due to density, inhibits ductal morphogenesis. Collectively, these findings reinforce the notion that matrix tension is a crucial regulator of cell morphogenesis.

The ability of a cell to contract and remodel the matrix is influenced by a balance between the stiffness of the matrix and cell contractility (Giannone and Sheetz, 2006; Larsen *et al*., 2006). Consistent with the finding that high-density gels are stiffer than low-density gels, T47D cells cultured 10 d in high-density floating gels contracted the gels 61% less than cells cultured in low-density floating gels (change in gel diameter, 6 mm in low-density vs. 2.33 mm in high-density gels) (Figure 1F). These results suggest that high-density gels are too stiff for cells to adequately contract. Floating gels did not contract when cells were absent (data not shown), verifying that gel contraction is a cell-mediated process.

Transduction of the physical properties of the ECM depends on myosin-mediated cell contractility (Pelham and Wang, 1997; Clark *et al*., 2007; Alexander *et al*., 2008). Furthermore, it has been shown that myosin II is critical for collagen fibril translocation and contraction of the collagen matrix through α2β1 integrin in fibroblasts (Meshel *et al*., 2005). Blebbistatin, an inhibitor of nonmuscle myosin II, disrupted tubule formation in low-density floating gels (Figure 1, G–J). Furthermore, treatment with blebbistatin reduced gel contraction by 55 and 50% in low- and high-density gels, respectively (Figure 1K). Interestingly, blebbistatin disrupted not only tubule formation but also the binding of cells to one another, suggesting that myosin-mediated contractility is necessary to maintain cell–cell junctions in this system. Thus, myosin-mediated gel contraction is necessary for cell–cell attachment as well as ductal morphogenesis, consistent with other findings that link cellular contractility to morphological regulation (Wozniak *et al*., 2003; Paszek *et al*., 2005; Engler *et al*., 2006; Guo *et al*., 2006; Fischer *et al*., 2009). Inhibition of gel contraction was not due to an effect on cell number, because blebbistatin did not inhibit cell proliferation (data not shown). These results suggest myosin is a key regulator of collagen matrix contraction in response to the stiffness of the ECM during ductal morphogenesis.

To determine whether myosin activity can be regulated by the density of the collagen matrix, we assessed myosin activity by using phosphospecific antibodies to MLC, which regulates the motor activity of myosin II (Adelstein and Eisenberg, 1980; Sellers *et al*., 1985). Phosphorylation of MLC correlates to an increase in contraction of actomyosin (Chrzanowska-Wodnicka and Burridge, 1996), and is an indication of activity, as phosphorylation of MLC on serine 19 is required for force production (Sellers *et al*., 1985; Umemoto *et al*., 1989), whereas additional phosphorylation at threonine 18 has been shown to enhance the actin-activated ATPase activity of myosin (Tanaka *et al*., 1985; Ikebe *et al*., 1986; Umemoto *et al*., 1989). Cells cultured in high-density gels exhibited an ~60% increase in monophosphorylated (Ser19) and a 45% increase in diphosphorylated (Thr18/Ser19) MLC (Figure 1L). However, even though the cells have increased pMLC levels in high-density gels, the elevated level of myosin activity was still not sufficient to contract these stiffer gels. Instead, it is probable that the cells have set up tension within the cell to balance the higher stiffness outside the cells, and this tension results in ongoing myosin activity. Conversely, that blebbistatin inhibits tubulogenesis suggests that myosin II is needed for the contraction of a compliant matrix. It is likely that myosin activity is tightly regulated during tubulogenesis, because pMLC levels are lower (but not absent) in a low-density collagen gel that is permissive for tubulogenesis to occur. Together, these results demonstrate the important balance that occurs between intracellular contractility and the stiffness of the matrix to regulate morphogenic processes.

Filamin A Levels Regulate Collagen Gel Contraction in Response to Matrix Stiffness

Filamin A binds to the cytoplasmic domain of β1 integrin and undergoes localization to integrin-induced adhesions in response to force application (Glogauer *et al*., 1998; D'Addario *et al*., 2002), suggesting FLNa may be an impor-

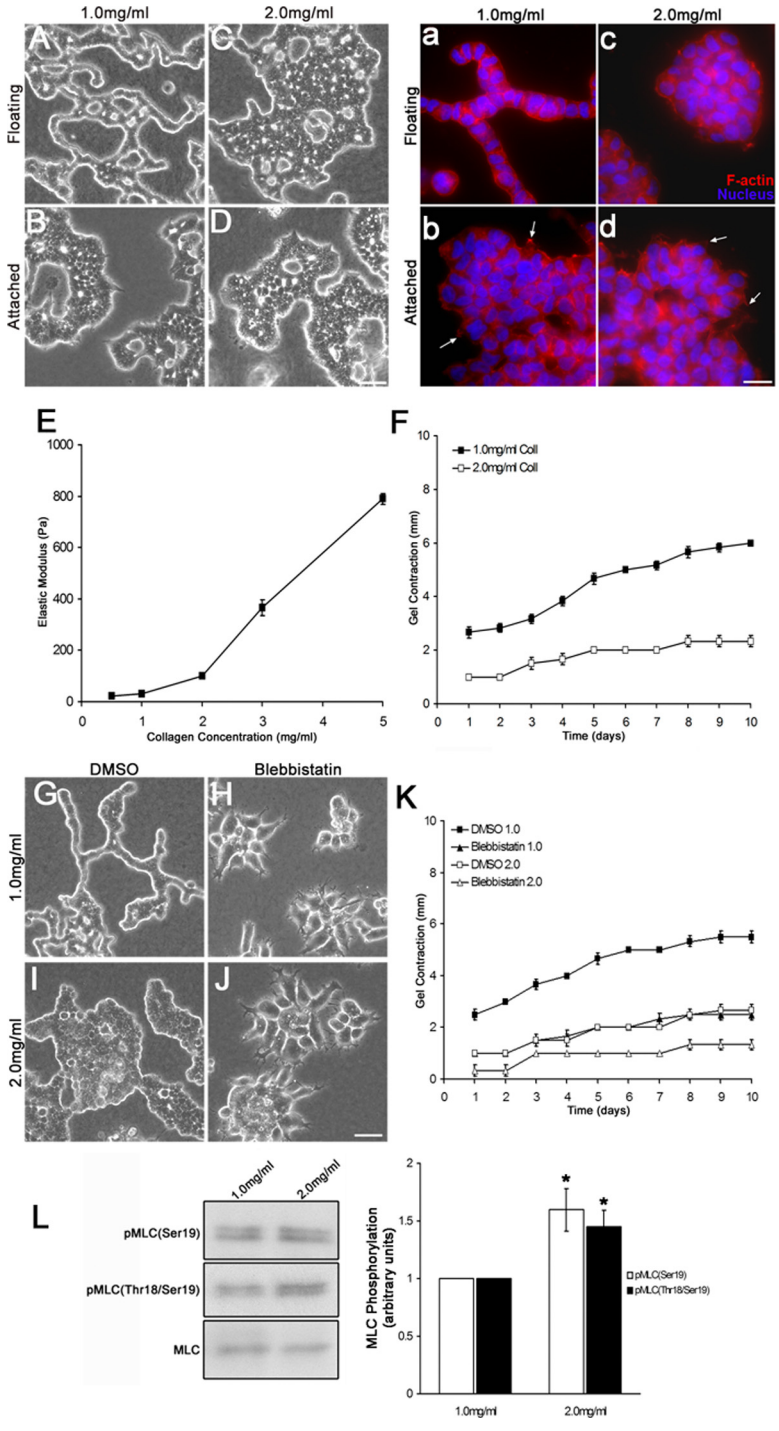

Figure 1. Cells must contract a compliant collagen matrix to undergo tubulogenesis. (A–D) T47D cells form tubules after 10 d when cultured in a compliant, low (1.0 mg/ml)-density floating collagen gel but not when the gel remains attached to the dish or when the collagen density is increased (2.0 mg/ml). Bar, 50 μm. (a–d) Fluorescent images of T47D cells in collagen gels labeled with AlexaFluor594 phalloidin (red) and bisbenzimide (blue). Bar, 20 μm. Cells exhibit protrusions in low- and high-density attached conditions (arrows), which is consistent with previous observations (Wozniak *et al.*, 2003). (E) Elastic modulus (ε) of cell-free collagen gels of increasing collagen concentration, measured by rheology as described in *Materials and Methods*. Collagen gels of greater concentration (density) have a stiffer elastic modulus. (F) Time course of gel contraction over 10 d. High-density gels are contracted 61% less than low-density gels at day 10. Statistics were performed on the mean contraction at day 10 from six experiments and demonstrated that contraction of a 2.0-mg/ml gel was statistically less than a 1.0-mg/ml gel (data not shown; $p < 0.001$ by a two-sample t test). (G–J) Actomyosin contractility is important for matrix contraction in response to collagen density. Blebbistatin (20 μM) disrupted tubule formation of T47D cells in low-density floating collagen gels. Bar, 50 μm. (K) Treatment with blebbistatin caused approximately a 55 and 50% reduction in the contraction of low- and high-density floating collagen gels at day 10, respectively, relative to dimethyl sulfoxide (DMSO) control for each collagen concentration. The mean contraction at day 10 from six independent experiments showed a statistically significant decrease in collagen gel contraction when blebbistatin was added to the culture compared with control cultures (data not shown; $p < 0.001$ by a two-sample t test). (L) Myosin activity is enhanced in cells cultured in high-density gels, as shown through Western blot analysis of MLC phosphorylation. pMLC(Ser19) increased by ~60%, whereas pMLC(Thr18/Ser19) was enhanced by ~45% in response to high-density gels. Left, representative Western blot. Right, data were graphed representing the mean ± SEM for eight experiments. *$p < 0.01$; statistical difference relative to low-density control (two-sample t test).

tant component of a mechanosensitive complex that couples the ECM to actomyosin contractility. Because breast epithelial cells respond to changes in the density of collagen gels, we determined the role of FLNa in collagen gel contraction. T47D cells were stably transfected with human FLNa shRNA, and knockdown was confirmed through immunoblotting (Figure 2A). Knockdown of hFLNa by shRNA resulted in a significant reduction in the contraction of low- and high-density gels (Figure 2B). The differences in gel contraction were not a result of changes in cell proliferation (data not shown). Moreover, FLNa knockdown correlated to an ~40% decrease in both pMLC(Ser19) and pMLC(Thr18/Ser19) levels (Figure 2E). These results suggest reduced FLNa expression reduces myosin activity and disrupts gel contraction.

To further explore the role of FLNa in matrix contraction, we used two approaches to increase FLNa expression in T47D cells. Knockdown of FILIP, which induces the degradation of filamin A, enhances endogenous FLNa expression in cortical neurons (Nagano *et al.*, 2002, 2004). T47D cells were stably transfected with FILIP shRNA, and increased FLNa expression was confirmed through immunoblotting (Figure 2C). Compared with control cells, FILIP shRNA significantly increased both the rate and extent of gel con-

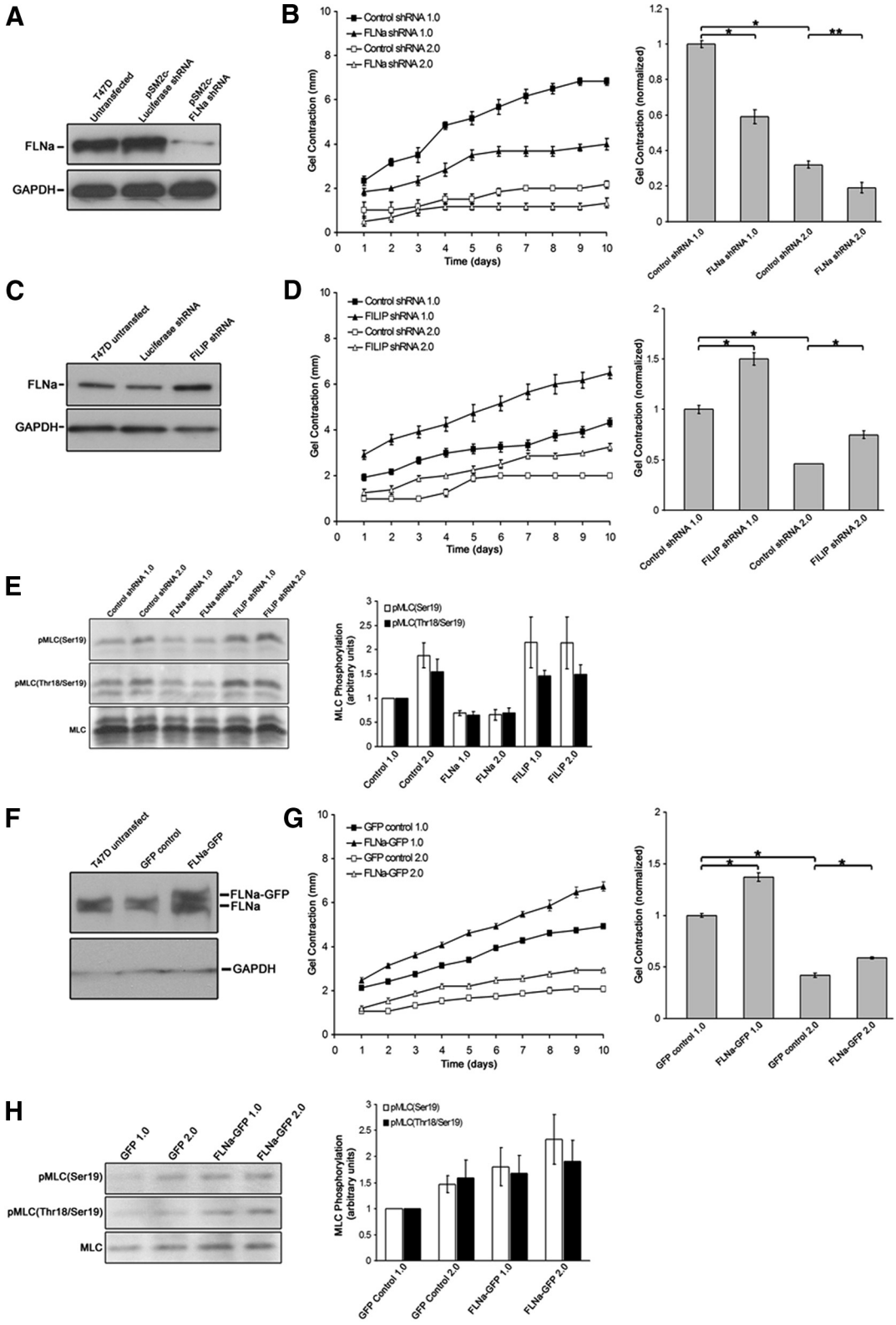

Figure 2. Filamin levels control the extent of collagen gel contraction and MLC phosphorylation. (A) Stable expression of FLNa shRNA reduced FLNa in T47D cells, demonstrated by Western blot analysis. GAPDH was used as a loading control. (B) Cells expressing FLNa shRNA exhibited a 42 and 38% reduction in gel contraction by day 10 when cultured in low- or high-density gels, respectively, relative to vector control for each collagen concentration. Data are represented over 10 d and are graphed as a mean for day 10 ± SEM for six experiments. *$p < 0.001$, **$p < 0.01$ statistical difference (two-sample *t* test). (C) Endogenous FLNa levels were increased by stably expressing FILIP shRNA, as demonstrated by Western blot with anti-FLNa antibodies. (D) Expression of FILIP shRNA increased gel contraction over 10 d, and by day 10 there was an increase of ~50 and 62% in low- and high-density floating gels, respectively, relative to control cells for

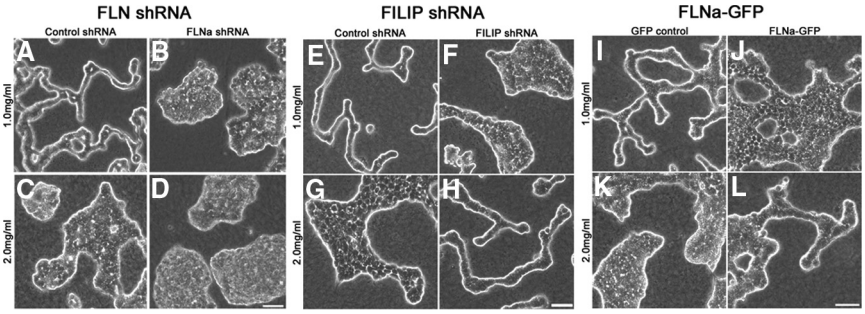

Figure 3. Filamin A levels tune tubulogenesis. (A–D) Expression of FLNa shRNA, which reduces endogenous FLNa expression, disrupted tubulogenesis in low-density floating gels (B vs. A). (E–H) Increased expression of endogenous FLNa by expressing FILIP shRNA disrupted tubulogenesis in low-density collagen gels but rescued tubulogenesis in high-density gels (H vs. G). (I–L) Expression of FLNa-GFP blocked tubule formation in low-density floating gels but rescued tubulogenesis in high-density floating gels. Bar (for all images), 50 μm.

traction (Figure 2D). Consistent with the observation that increased FLNa enhanced gel contraction, these cells also exhibited increased pMLC(Ser19) and pMLC(Thr18/Ser19) (Figure 2E).

Knockdown of FILIP, while increasing filamin A expression, also may have other unknown effects on matrix remodeling and tubulogenesis unrelated to enhanced FLNa levels. Therefore, as a complimentary approach, GFP-labeled FLNa was overexpressed in T47D cells. Levels of GFP in both control GFP cells and FLNa-GFP cells were comparable, as measured using flow cytometry (data not shown). Immunoblot analysis verified endogenous FLNa levels were similar in GFP control and FLNa-GFP cells, whereas expression of FLNa-GFP increased the total level of FLNa (endogenous FLNa + FLNa-GFP) by approximately twofold (Figure 2F). Expression of FLNa-GFP significantly enhanced both the rate and extent of gel contraction (Figure 2G) and correlated to an increase in both pMLC(Ser19) and pMLC(Thr18/Ser19) in both low- and high-density gels (Figure 2H). It is important to note that increasing FLNa expression, using either approach (FILIP shRNA or expression of FLNa-GFP), enhanced pMLC above that observed in control cells (Figure 2, E and H). The increased contraction of both FILIP shRNA and FLNa-GFP cell lines was not due to changes in cell proliferation (data not shown). These results suggest that increased FLNa expression supports increased myosin light chain phosphorylation, thus facilitating gel contraction in high-density gels.

Figure 2 (cont). each collagen concentration. Bar graphs represent the mean ± SEM for at least eight experiments. *$p < 0.001$ statistical difference (two-sample *t* test). (E) Perturbing FLNa levels down or up regulates myosin activity, as measured by pMLC. T47D cells expressing FLNa shRNA exhibited a 65–70% reduction in pMLC(Ser19) and pMLC(Thr18/Ser19), whereas FILIP shRNA-expressin cells exhibited a 45–115% increase in pMLC(Ser19) and pMLC(Thr18/Ser19) in both low- and high-density gels. Note that increased FLNa expression enhanced pMLC above that observed in control cells. Graphed data represent the mean ± SEM for at least six experiments. $p < 0.05$ for all cell types and conditions; statistical difference compared with low-density control (two-sample *t* test). (F) Overexpression of FLNa-GFP in T47D cells was confirmed by Western blot analysis. Expression of FLNa-GFP did not alter expression of endogenous FLNa. (G) Expression of FLNa-GFP enhances matrix contraction. FLNa-GFP enhanced gel contraction in both low and high-density floating gels, similar to FILIP shRNA. Data expressed over 10 d and graphed at day 10, representing the mean ± SEM for 15 experiments. *$p < 0.001$ statistical difference (two-sample *t* test). (H) Cells expressing FLNa-GFP exhibit increased pMLC(Ser19) and pMLC(Thr18/Ser19) levels in both low and high-density gels. Note that expression of FLNa-GFP enhanced pMLC above that observed in control cells. Graphs represent the mean from 10 experiments ± SEM $p < 0.05$ for all experimental conditions; statistical significance relative to low-density control (two-sample *t* test).

Filamin A Levels Tune Tubulogenesis in Stiffer Collagen Gels

The observation that the level of FLNa affected matrix contraction and phosphorylation of MLC suggested that FLNa might regulate the ability of cells to adjust to stiffer matrix environments. To determine whether this was the case, we determined the effects of modulating FLNa levels on tubulogenesis. Knockdown of hFLNa by shRNA disrupted tubule formation in low-density floating collagen gels (Figure 3B), supporting the important role FLNa plays in this process. As a control, T47D cells stably transfected with luciferase shRNA exhibited normal phenotypes in both low- and high-density gels (Figure 3, A and C), meaning that they formed tubules in low-density gels but not in high-density gels. Importantly, when endogenous FLNa levels were increased by expression of FILIP shRNA, tubulogenesis occurred in the stiffer 2.0 mg/ml collagen gels (Figure 3H). The same result was observed when FLNa levels were increased by expression of FLNa-GFP (Figure 3L). It was of interest that increased FLNa levels disrupted tubulogenesis in the compliant 1.0 mg/ml collagen gels (Figure 3, F and J), again suggesting that it is the balance of contractile forces within the context of the matrix compliance that regulates cellular behavior, controlling morphogenesis. Because of these results, note that we do not include here "rescue" of FLNa shRNA-expressing cells by re-expressing FLNa, because changes in FLNa levels due to re-expression affect the outcome and make the experiments difficult to interpret.

Filamin a-β1 Integrin Interactions Are Regulated by Collagen Density

β1 integrin is an important regulator of breast epithelial cell morphogenesis in reconstituted matrices in vitro and in the mammary gland in vivo (Keely *et al*., 1995; Zutter *et al*., 1995; Weaver *et al*., 1997; Chen *et al*., 2002; White *et al*., 2004; Naylor *et al*., 2005). Because FLNa binds to the cytoplasmic domain of β1 integrin and accumulates at adhesion sites in response to mechanical tension (Glogauer *et al*., 1998; Loo *et al*., 1998; Pfaff *et al*., 1998; D'Addario *et al*., 2002), we determined whether the density of the matrix can regulate FLNa binding to β1 integrin. FLNa-β1 integrin coprecipitation was enhanced in T47D cells cultured in high-density collagen gels (Figure 4A). Although culture of cells in low-density attached gels enhanced FLNa-β1 integrin association by ~56% compared with low-density floating gels, culture in either high-density floating or attached gels produced a 96 and 103% increase in FLNa-β1 integrin association, respectively (Figure 4A). These results suggest FLNa binding to β1 integrin is enhanced in a stiffer matrix.

Although increased levels of FLNa enhanced contraction of collagen gels (Figure 2), it is unclear whether this effect on contraction is due to enhanced FLNa-β1 interactions or to other functions of FLNa. Therefore, we first determined

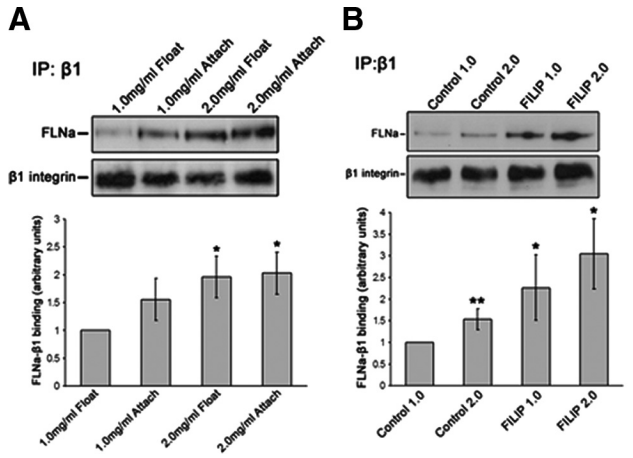

Figure 4. Increased collagen density regulates FLNa-β1 integrin interactions. (A) Coimmunoprecipitation (IP) of T47D cells cultured in low- or high-density collagen gels. Cells in high-density gels exhibited a 96 and 103% increase compared with cells in low-density gels in FLNa binding to β1 integrin in floating or attached gels, respectively. Graphed data represent the mean ± SEM for five experiments. (B) Overexpression of FLNa by using FILIP shRNA increased FLNa-β1 integrin interactions that were not regulated by collagen density. Although control cells displayed ~66% increase in FLNa-β1 integrin interactions in high-density floating gels compared with low-density gels, FILIP shRNA further enhanced FLNa binding to β1 integrin by ~160 and 240% in low- and high-density floating gels, respectively. Graphed data represent the mean ± SEM for four experiments. *$p < 0.05$, **$p < 0.01$; statistical difference relative to low-density control gels (two-sample *t* test). Immunoglobulin G control for IPs is found in Supplemental Figure 1.

whether cells expressing elevated levels of FLNa exhibit enhanced FLNa-β1 integrin interactions in response to changes in collagen density. Using T47D FILIP shRNA cells, we observed that FLNa-β1 integrin interactions were enhanced by ~160 and 240% in low- and high-density floating collagen gels, respectively (Figure 4B). These results suggest that the FLNa-β1 integrin interaction may mediate the elevated collagen gel contraction noted in Figure 2 for FILIP shRNA-expressing cells. Note that on a quantitative level, the relative amount of FLNa/β1 integrin is higher in cells expressing FILIP shRNA than in parental T47D cells cultured in a high-density 2.0 mg/ml gel. This suggests that, even though cells respond to a stiffer matrix by increasing FLNa association with β1 integrin, this interaction may still not be enough to rescue tubulogenesis of parental cells in the high-density gels.

FLNa Binding to β1 Integrin Mediates the Effects of FLNa on Collagen Matrix Contraction and Tubulogenesis

In addition to directly binding to β1 integrin, FLNa binds to several proteins in the cytosol (Stossel *et al*., 2001). Thus, it is possible that up or down-regulation of FLNa levels affects several pathways. To determine whether it is the specific binding of FLNa to β1 integrin that influences gel contraction and morphogenesis, we competitively inhibited endogenous FLNa binding to β1 integrin by overexpressing domain 21 of FLNa, which contains the integrin-binding region (Loo *et al*., 1998; Kiema *et al*., 2006). T47D cells were transfected with enhanced EGFP-IgFLNa21 (termed GFP-F21) to compete with endogenous FLNa for binding to β1 integrin. As a control, T47D cells were transfected with EGFP-IgFLNa21(I/C) (termed GFP-F21(I/C)) containing a point mutation at Ile2283 that impairs β1 integrin binding (Kiema *et al*., 2006). This fragment is an appropriate control because it does not bind to β1 integrin and does not block FLNa-β1 integrin interactions. Fluorescence-activated cell sorting (FACS) analysis was carried out to isolate cells expressing equal levels of GFP-F21(I/C) and GFP-F21 (data not shown). Expression of GFP-F21(I/C) or GFP-F21 did not alter endogenous FLNa expression in these cells (Figure 5A). Cells expressing GFP-F21 displayed reduced levels of binding between endogenous FLNa and β1 integrin in both low- and high-density collagen gels (Figure 5B), whereas GFP-F21(I/C) cells showed "normal" FLNa-β1 integrin interactions that were increased in high-density gels relative to low density gels, consistent with untransfected T47D cells (Figure 4A). Expression of GFP-F21 diminished gel contraction compared with control GFP-F21(I/C) cells (Figure 5C). By day 10, GFP-F21 cells exhibited a 26 and 28% reduction in gel contraction in low- and high-density gels, respectively, supporting the idea that FLNa-β1 integrin interactions regulate gel contraction. Expression of IgFLNa21 blocked the density-dependent increases in pMLC(Ser19) and pMLC(Thr18/Ser19) (Figure 5D). These results suggest that reducing FLNa-β1 integrin interactions reduces collagen matrix contraction and activation of myosin.

Consistent with our finding that contraction, FLNa, and tubulogenesis are linked, blocking FLNa-β1 integrin interactions with IgFLNa21 disrupted tubulogenesis (Figure 5I). In contrast, control IgFLNa21(I/C) cells formed tubules in low-density gels (Figure 5G). All cell types exhibited disrupted tubule formation when cultured in high-density collagen gels (Figure 5, F, H, and J). Thus, FLNa binding to β1 integrin mediates the effects of FLNa on tubulogenesis.

Increased Binding of FLNa to β1 Integrin Enhances Collagen Matrix Contraction and Tunes Tubulogenesis in a Stiffer Collagen Matrix

Reduction of FLNa-β1 integrin binding disrupted gel contraction and tubulogenesis (Figure 5). Therefore, we next determined whether enhanced FLNa-β1 integrin interactions also regulate matrix contraction and morphogenesis. To do this, we used a human β1 integrin containing two point mutations (V787,791I) in the cytoplasmic domain filamin-binding site that enhance FLNa binding (Calderwood *et al*., 2001). This mutant β1 integrin, hβ1(V787,791I), was stably expressed in NMuMG cells. Because hβ1(V787,791I) integrin was expressed in mouse NMuMG cells, we were able to identify and select cells that express the human form of β1 integrin using a human-specific β1 integrin antibody. As a control, wild-type human β1 [hβ1(WT)] integrin was stably expressed in NMuMG cells to similar levels as hβ1(V787,791I), which was confirmed using FACS analysis (data not shown). Expression of hβ1(WT) or hβ1(V787,791I) integrin did not affect the expression of FLNa in NMuMG cells (Figure 6A). For this set of experiments, it should be noted that NMuMG cells, which have an increased ability to contract collagen matrices compared with T47D cells, require a higher density of collagen matrix relative to T47D cells to undergo branching morphogenesis, and thus 2.0 mg/ml is a compliant matrix for these cells, whereas 3.0 mg/ml is a stiff matrix. hβ1(V787,791I) integrin exhibited a 147 and 152% increase in binding to mouse FLNa in both 2.0 and 3.0 mg/ml floating collagen gels, respectively, as determined by coimmunoprecipitation with β1 integrin (Figure 6B).

To test whether expression of hβ1 integrin affects gel contraction by NMuMG cells, we compared both hβ1(WT) and hβ1(V787,791I) cell lines with untransfected NMuMG

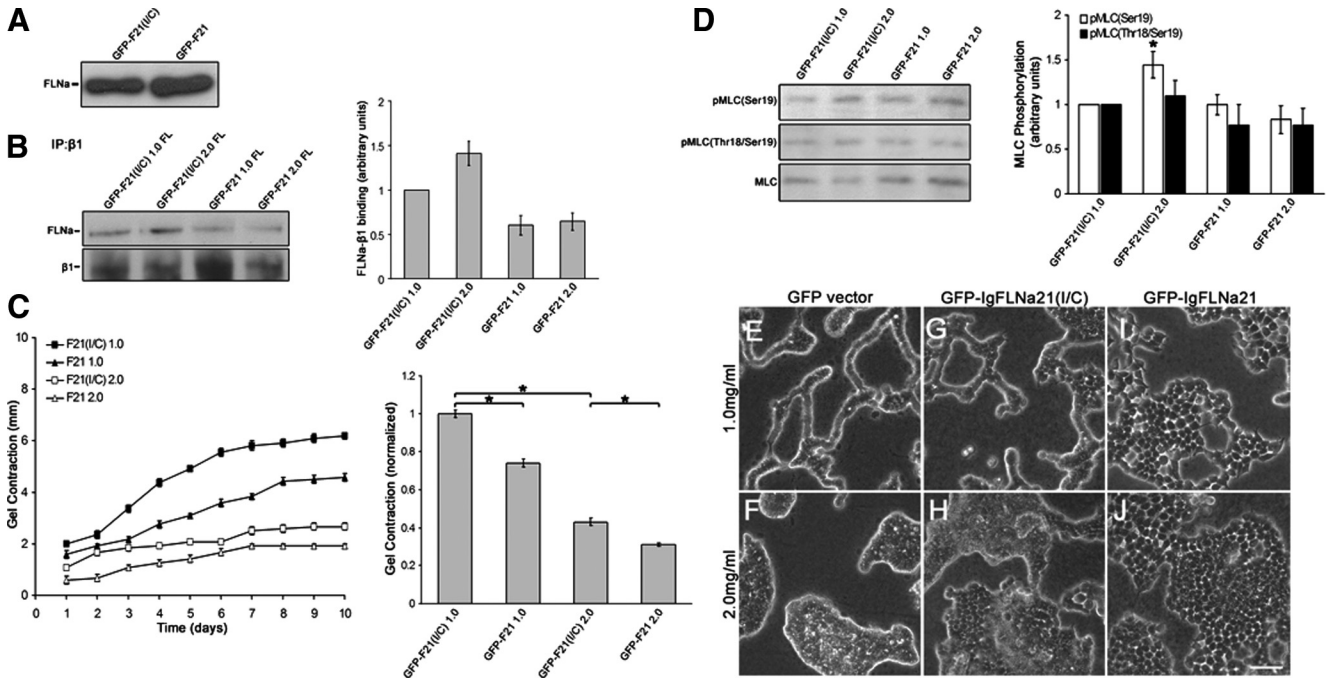

Figure 5. Decreased FLNa-β1 integrin binding reduces collagen matrix contraction and disrupts tubule formation. To inhibit FLNa-β1 integrin interactions, the integrin-binding region of FLNa coupled to GFP (GFP-F21) was expressed in T47D cells. As a control, the same construct containing a point mutation that abolishes FLNa binding to β1 integrin, GFP-F21(I/C), was used. (A) T47D cells expressing GFP-F21(I/C) or GFP-F21 have similar levels of endogenous FLNa, demonstrating that these constructs do not alter FLNa levels. Equal numbers of cells were lysed and used for comparison of FLNa expression. (B) Coimmunoprecipitation with anti-β1 integrin antibody demonstrates that GFP-F21, which binds to β1 integrin, reduced coprecipitation of FLNa with β1 integrin, whereas GFP-F21(I/C), which does not bind β1 integrin, did not block FLNa-β1 integrin coprecipitation. Graphed data (right) represent the mean of three similar experiments quantified ± SEM, $p < 0.05$ for all conditions; statistical significance relative to GFP-F21(I/C) control cells in low-density collagen gels (two-sample *t* test). (C) Disruption of FLNa binding to β1 integrin reduces contraction of collagen gels. Compared with GFP-F21(I/C) controls, GFP-F21 cells display a 26 and 28% reduction in the contraction of low- and high-density floating gels, respectively, at day 10. Bar graph data represent the mean contraction at day 10 ± SEM from a minimum of 11 experiments. *$p < 0.001$ statistical difference (two-sample *t* test). (D) Expression of GFP-F21 blocked the density-dependent increase in both pMLC(Ser19) and pMLC(Thr18/Ser19). However, GFP-F21 did not have a significant effect on pMLC levels in low-density gels. Quantified data represent the mean ± SEM for seven experiments. *$p < 0.02$; statistical difference compared with control cells in low-density collagen gels (two-sample *t* test). (E–J) Cells expressing GFP-F21(I/C) formed tubules in low-density collagen gels and exhibited disrupted tubulogenesis in high-density floating gels, similar to GFP vector control. However, expression of GFP-F21 disrupted tubulogenesis in both low- and high-density floating gels. Bar, 50 μm.

cells in 2.0 mg/ml collagen gels. Expression of hβ1(WT) slightly increased gel contraction compared with untransfected cells (Figure 6C). In contrast, expression of hβ1(V787,791I) integrin significantly enhanced contraction of 2.0 mg/ml collagen gels (Figure 6C). By culture day 4, expression of hβ1(V787,791I) integrin enhanced gel contraction by 85% compared with hβ1(WT) cells. The differences in gel contraction were not due to changes in proliferation (data not shown). Consistent with enhanced gel contraction, expression of hβ1(V787,791I) increased mono- and diphosphorylated MLC in both low and high-density gels (Figure 6D).

NMuMG-hβ1(WT) cells displayed a similar degree of branching morphogenesis as untransfected NMuMG cells when cultured in low-density collagen gels (Figure 6, E and F). Note that NMuMG cells form branching structures that differ from T47D cells, which we think relates to their increased contractile phenotype. In contrast, cells expressing hβ1(V787,791I) integrin lost the ability to undergo branching morphogenesis in 2.0 mg/ml collagen gels (Figure 6G). Because hβ1(V787,791I)-expressing cells have an enhanced ability to contract collagen gels, similar to cells that overexpress FLNa, we determined whether increasing collagen density could tune branching morphogenesis in these cells. Increasing the collagen density to 3.0 mg/ml was sufficient for hβ1(V787,791I)-expressing cells to now undergo branching morphogenesis (Figure 6H). Thus, consistent with FLNa overexpression, enhancing FLNa-β1 integrin interactions through expression of hβ1(V787,791I) disrupted morphogenesis in more compliant gels by shifting the balance of gel contraction. However, increasing the stiffness of the matrix by culturing these cells in higher density gels was sufficient to counterbalance the effect of increased FLNa-β1 integrin interactions to tune branching morphogenesis.

Filamin-β1 Integrin Regulates Collagen Gel Remodeling

Our results suggest that tubulogenesis occurs only when cells are in a matrix that is compliant enough for the cells to contract it and that tuning the contractile response through FLNa binding to β1 integrin allows cells to form tubules in gels that are stiffer. When cells contract a collagen matrix, they remodel the individual collagen fibrils and translocate the fibrils toward the cells, resulting in condensed regions of collagen surrounding cell bodies (Yamato *et al*., 1995; Tamariz and Grinnell, 2002; Miron-Mendoza *et al*., 2008). Therefore, we next examined the fate of the collagen fibrils as a consequence of the remodeling that occurs during tubulogenesis. To investigate how collagen fibers are reorganized during tubulogenesis, we used multiphoton laser scanning micros-

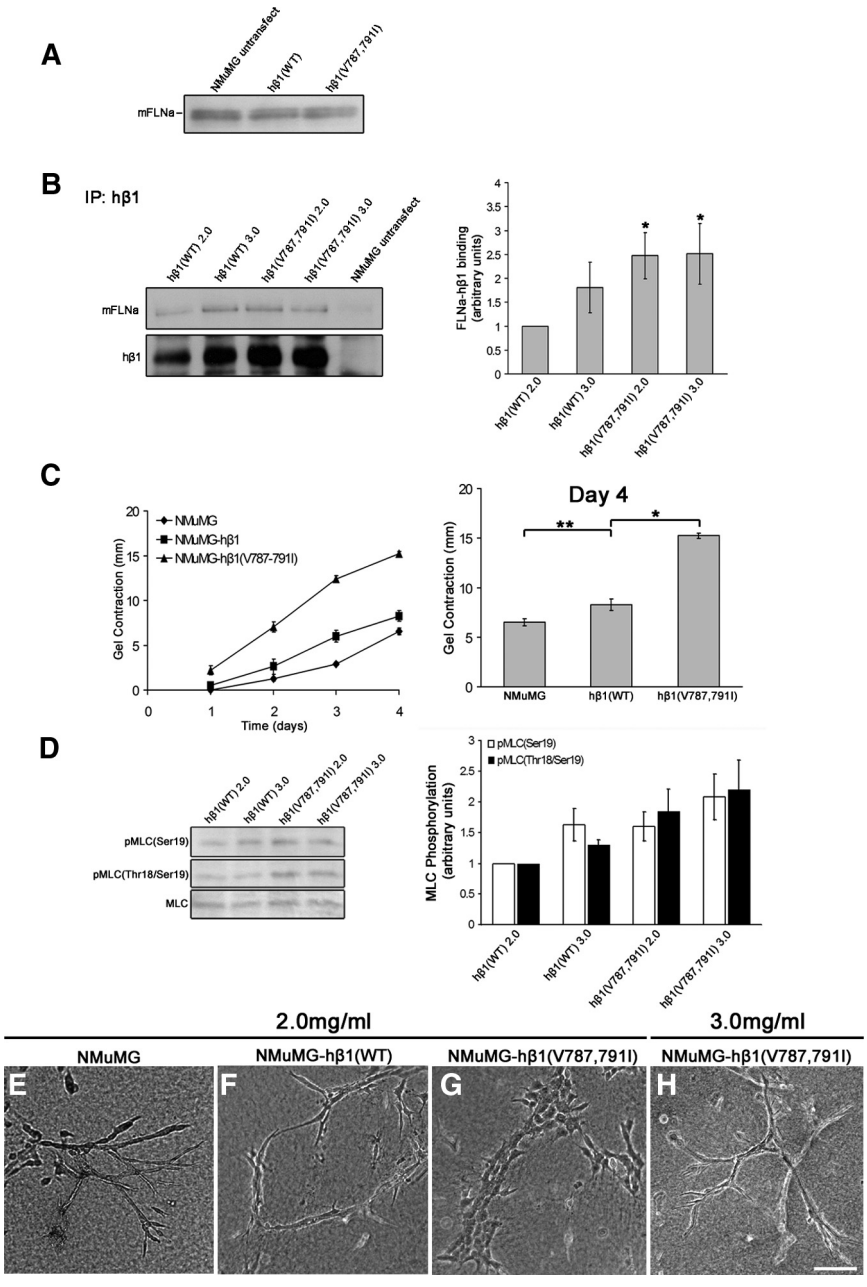

Figure 6. Increased FLNa binding to β1 integrin enhances matrix contraction and tunes branching morphogenesis. Mouse NMuMG cells were stably transfected with human β1 integrin wild-type (WT) or a β1 integrin containing two point mutations that specifically enhance binding of FLNa, hβ1(V787,791I). (A) Western blot of lysates from NMuMG cells expressing either hβ1(WT) or hβ1(V787,791I) demonstrates that these constructs did not alter levels of FLNa. Equal numbers of cells were lysed and used for comparison of mFLNa expression. (B) Cells expressing hβ1(V787,791I) cells have enhanced mFLNa binding to hβ1 integrin in both low- (2.0 mg/ml) and high (3.0 mg/ml)-density gels, whereas WT hβ1 integrin binding to mFLNa is regulated by matrix density. Immunoprecipitations (IPs) were performed with anti-hβ1 integrin antibody, the specificity of which was verified using equal numbers of untransfected NMuMG cells that do not express hβ1 integrin. Quantified data represent the mean ± SEM for four experiments. *$p < 0.05$; statistical difference compared with low-density control (two-sample *t* test). (C) Enhanced FLNa-β1 integrin interactions enhanced collagen gel contraction, shown over 4 d (left). Expression of hβ1(V787,791I) enhanced levels of gel contraction at day 4 relative to both hβ1(WT) and untransfected cells (right). Data are mean ± SEM from a minimum of eight experiments. *$p < 0.001$, **$p < 0.05$ statistical difference (two-sample *t* test). (D) Expression of hβ1(V787,791I) enhanced pMLC(Ser19) and pMLC(Thr18-Ser19) in both low- and high-density collagen gels. Quantified data represent the mean ± SEM for five experiments. $p < 0.05$ for all conditions; statistical significance relative to low-density hβ1 integrin control (two-sample *t* test). (E–H) Increased FLNa binding to β1 integrin tunes branching morphogenesis in high-density gels. Although NMuMG-hβ1(WT) cells exhibited a branched phenotype in low (2.0 mg/ml)-density gels (F), hβ1(V787–791I) cells exhibited disrupted morphogenesis in low-density gels (G). However, increasing the collagen density to 3.0 mg/ml was sufficient for hβ1(V787-791I) cells to undergo branching morphogenesis (H). Bar, 100 μm.

copy (MPLSM) (Denk *et al*., 1990) and SHG imaging (Campagnola and Loew, 2003) to directly observe the rearrangement of type I collagen under matrix conditions that facilitate cell morphogenesis. Because collagen is noncentrosymmetric, we can use SHG to examine the orientation and density of fibrillar collagen without the need for indirect labeling using fluorescently tagged proteins or antibodies (Mohler *et al*., 2003; Provenzano *et al*., 2006). Moreover, the intensity of the SHG signal corresponds in a linear manner to collagen concentration (Brown *et al*., 2003; Mohler *et al*., 2003).

Using MPLSM and SHG, we visualized cell–ECM boundaries to examine the local organization of the collagen matrix under conditions that facilitate breast epithelial cell morphogenesis. Collagen gels without cells exhibited randomly organized collagen fibrils (Figure 7, A and B). Consistent with previous studies, increasing the collagen concentration increased the density of visible collagen fibrils (Roeder *et al*., 2002) and increased the intensity of the collagen SHG signal (Figure 7, A vs. B). When T47D cells were added to low-density floating gels, collagen fibrils were relocalized into condensed regions between and directly adjacent to tubular structures, as indicated by an increase in fluorescence intensity (Figure 7, C and E). Interestingly, this resulted in a local collagen matrix with a greater concentration than the high-density gels, which again suggests that it is not collagen ligand density per se to which cells respond when comparing a low-density gel to a high-density gel. Rather, these results suggest it is the tension of the matrix in which the cell resides that determines subsequent cellular behavior. In contrast, condensation of collagen fibrils in high-density floating gels was diminished and limited to regions immediately adjacent to the cell structures (Figure 7, D and F), consistent with the limited amount of global gel contraction observed

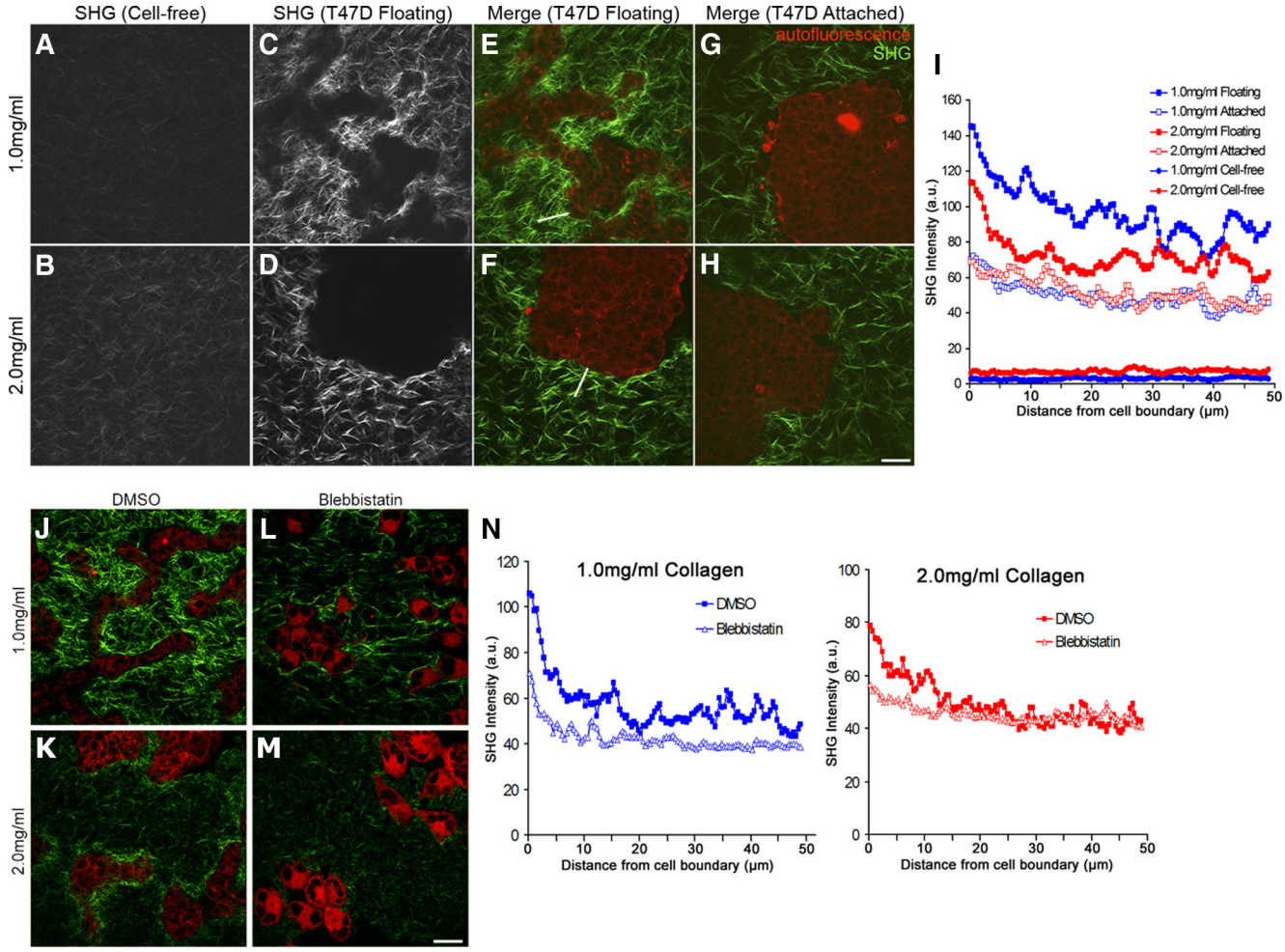

Figure 7. Establishment of a quantitative assay demonstrates that collagen gel remodeling occurs via contractility. Representative SHG images of low (1.0 mg/ml) and high (2.0 mg/ml) density collagen gels showing random fibril organization of cell-free gels (A and B) compared with floating gels of the same concentration containing cells (C and D). (E–H) MPLSM/SHG merged images of collagen (green) and T47D cell autofluorescence (red) in floating and attached gels of low (1.0 mg/ml) and high (2.0 mg/ml) density. White lines in E and F are examples of a region of interest where SHG fluorescence intensity was measured along line scans and used for data presented in I. Bar, 50 μm. (I) Average SHG fluorescence intensity of collagen fibrils in low and high-density gels. Line scans 50 μm in length were drawn from the edge of the cell–ECM boundary (=0 μm) into the collagen gel and graphed as a function of distance from the edge of the cell. For empty gels, line scans of 50 μm were taken randomly throughout the image. Data represent nine images, three measurements per image, averaged. At 5 μm out from the cell boundary, statistical difference $p < 0.001$ (1.0 floating vs. 2.0 floating; 2.0 floating vs. 1.0 attached; 2.0 floating vs. 2.0 attached) by the two-sample *t* test. By regression analysis, $p < 0.0001$ (1.0 floating vs. 2.0 floating) for each line scan. (J–M) Representative images of collagen (green) and cell autofluorescence (red) show diminished collagen fibril condensation in both low- (1.0 mg/ml) and high (2.0 mg/ml)-density floating collagen gels in the presence of blebbistatin. Bar, 50 μm. (N) Average intensity of collagen fluorescence taken from the edge of the cell–ECM boundary (=0 μm) out 50 μm into the collagen matrix in low- and high-density gels. Data are averaged from a minimum of eight images, three measurements per image. $p < 0.01$ statistical difference (1.0 DMSO vs. 1.0 blebbistatin), $p < 0.05$ (2.0 DMSO vs. 2.0 blebbistatin) at 5 μm out by two-sample *t* test. By regression analysis, $p < 0.0001$ (1.0 vs. 1.0 + blebbistatin; and 2.0 vs. 2.0 + blebbistatin) for each line scan.

for dense gels (Figure 2). Notably, morphogenesis did not occur in high-density gels, strengthening the link between collagen gel contraction leading to matrix reorganization and tubulogenesis (Wozniak *et al.*, 2003).

To quantify collagen rearrangement, a region of interest along a line scan was used to measure the collagen fluorescence intensity from the edge of the cell–ECM boundary (0 μm) out 50 μm into the collagen matrix. Although the entire gel had been reorganized in the presence of cells, these measurements indicate collagen condensation was most enhanced within 15 μm of the cell boundary in floating gels (Figure 7I). Consistent with the global gel contraction results, collagen fibril condensation is cell dependent, because no collagen fibril condensation occurred when cells were absent in floating gels (note flat lines in Figure 7I). Importantly, changes in collagen fluorescence intensity were more robust in low-density floating gels relative to high-density floating gels, consistent with the observation that there was also quantitatively more global gel contraction in low-density gels (compare with Figure 1F). Although gel contraction is not possible in attached gels due to the nature of the assay, it is interesting to note that some reorganization did occur in attached gels of both low- and high-density, although this was much less than that observed in floating collagen gels, and collagen fibrils did not condense near regions adjacent to cell structures (Figure 7, G and H).

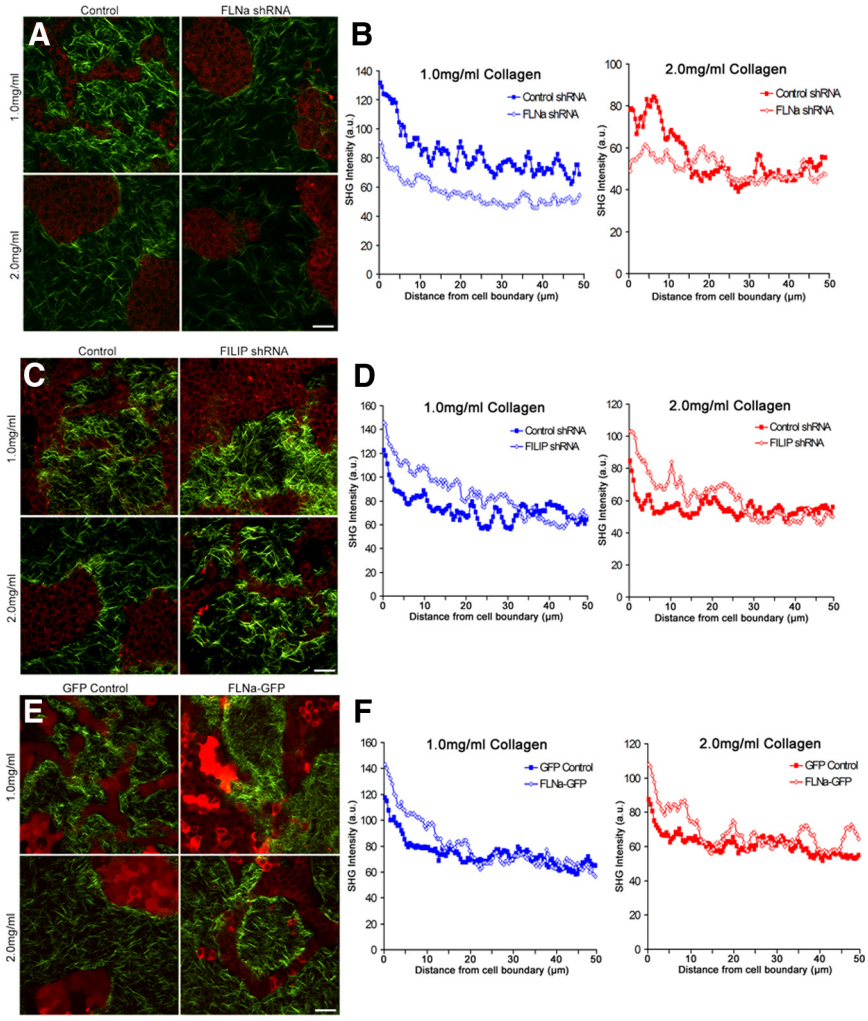

Figure 8. FLNa levels regulate collagen matrix remodeling. (A) FLNa shRNA reduces collagen fibril condensation and matrix reorganization. Collagen (green) and cell autofluorescence (red) were imaged using SHG and MPLSM, respectively. Bar, 50 μm. (B) Line scan of SHG images represented in A to quantify the fluorescence intensity taken from the edge of the cell–ECM boundary (0 μm) into the collagen matrix of low- and high-density floating gels. Data are averaged from a minimum of six images, three measurements per image. At 5 μm, statistical difference $p < 0.01$ (1.0 control vs. 1.0 FLNa shRNA), $p < 0.05$ (2.0 control vs. 2.0 FLNa shRNA)(two-sample t test) and $p < 0.0001$ by regression analysis. (C) FILIP shRNA enhances collagen fibril condensation. Cell autofluorescence (red) and collagen (green) were imaged using MPLSM and SHG imaging, respectively. Bar, 50 μm. (D) Average fluorescence intensity of collagen fibrils in low- and high-density floating gels. Line scans were taken from the edge of the cell–ECM boundary (0 μm) into the collagen matrix. Data are averaged from a minimum of six images, three measurements per image. $p < 0.05$ statistical difference at 5 μm (1.0 control vs. 1.0 FILIP shRNA; 2.0 control vs. 2.0 FILIP shRNA) (two-sample t test), and $p < 0.0001$ by regression analysis. (E) FLNa-GFP enhances collagen fibril condensation near cell structures. GFP-labeled cells (pseudocolored red) and collagen (green) were imaged using MPLSM and SHG imaging, respectively. Bar, 50 μm. (F) Fluorescence intensity measurements were taken from the edge of the cell–ECM boundary (0 μm) into the collagen matrix of low and high-density floating gels. Data are averaged from a minimum of eight images, three measurements per image. At 5 μm, statistical difference $p < 0.05$ (1.0 GFP control vs. 1.0 FLNa-GFP; 2.0 GFP control vs. 2.0 FLNa-GFP) (two-sample t test), and $p < 0.0001$ by regression analysis.

To verify that the collagen fibril remodeling and condensation was due to contractile forces, cultures were treated with blebbistatin to inhibit myosin II activity. Blebbistatin treatment reduced the extent of collagen fibers that condensed near cell–ECM boundaries (Figure 7, J–N). These results support previous studies suggesting that gel contraction involves collagen fibril condensation toward cells (Yamato *et al*., 1995; Tamariz and Grinnell, 2002; Meshel *et al*., 2005; Miron-Mendoza *et al*., 2008) and further links matrix contraction and remodeling to tubule formation in compliant 3D collagen gels.

To determine the role of FLNa levels in matrix remodeling, collagen fiber condensation was quantified for cells with increased and decreased FLNa levels. FLNa shRNA diminished the ability of cells to reorganize the matrix as measured using SHG (Figure 8A). Analysis of fluorescence intensity along line scans confirmed the reduction of collagen fibrils that condensed near cell boundaries when FLNa expression was reduced (Figure 8B). Conversely, increased FLNa expression in cells expressing FILIP shRNA enhanced their ability to condense collagen around cell structures, as noted by SHG fluorescence in both low- and high-density gels (Figure 8C). Average fluorescence intensity measurements confirmed an increase in the condensation of collagen fibrils adjacent to cell-ECM boundaries in FILIP shRNA-expressing cells (Figure 8D), supporting the idea that increased FLNa increases collagen gel contraction. Overexpression of FLNa-GFP also enhanced the condensation of collagen fibrils adjacent to cell–ECM boundaries in both low- and high-density gels (Figure 8, E and F).

Collagen fibril remodeling was not only regulated by FLNa levels, but specifically by interaction of FLNa with β1 integrin, because expression of the FLNa-β1 integrin blocking peptide GFP-F21 diminished collagen fibril condensation (Figure 9, A–D). Conversely, enhanced interaction of FLNa with β1 integrin enhanced the ability of the cells to remodel and condense the collagen fibers (Figure 9, E–H). Most notably, although NMuMG cells expressing hβ1(WT) integrin could only minimally condense collagen fibers in a high-density gel (Figure 9F), expression of hβ1 (V787,791I) integrin dramatically increased condensation of collagen fibers, even in a high-density gel (Figure 9H). Collectively, these data imply that an optimal level of gel contraction and remodeling is necessary for tubulogenesis to occur in a specified matrix density, and that enhancing gel contraction by enhancing FLNa-β1 integrin interactions tunes the cellular response in higher density gels, resulting in collagen fiber rearrangements and rescuing morphogenesis in high-density gels.

DISCUSSION

The compliance of the ECM and cellular regulation of matrix remodeling are critical determinants of tissue morphogene-

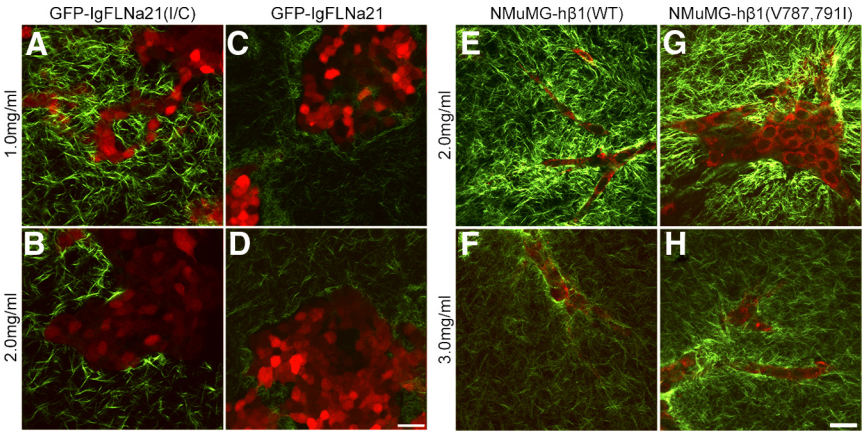

Figure 9. The interaction of FLNa with β1 integrin regulates collagen matrix remodeling. (A–D) GFP-F21 reduced the ability of cells to reorganize the collagen matrix, compared with control cells expressing GFP-F21(I/C). GFP-labeled cells (pseudocolored red) and collagen (green) were imaged using MPLSM and SHG imaging, respectively. Bar, 50 μm. Line scans (not shown) taken from the edge of the cell–ECM boundary from 6 images, three measurements per image demonstrated that there is a statistical difference between 1.0 GFP-F21(I/C) versus 1.0 GFP-F21, $p < 0.05$ by two-sample t test and by regression analysis. (E–H) FLNa binding to β1 integrin was enhanced in NMuMG cells by expression of human β1 integrin containing two point mutations that specifically enhance binding of FLNa, hβ1(V787,791I). Expression of hβ1 integrin wild type (WT) served as a control. Note that increased FLNa-β1 integrin interactions in hβ1(V787,791I) enhanced matrix remodeling compared with hβ1(WT) even in the high-density (3.0 mg/ml) collagen gel.

sis. This study demonstrates that FLNa binding to β1 integrin is an important regulator of matrix contraction during breast epithelial cell morphogenesis. We show that increased collagen density results in a stiffer matrix that regulates cell morphogenesis, gel contraction, and FLNa-β1 integrin interactions. Interaction of FLNa with β1 integrin is important for these processes, because disruption of FLNa-β1 integrin complexes disrupts collagen gel contraction and morphogenesis. Conversely, increasing FLNa-β1 integrin interactions enhances gel contraction and allows cell morphogenesis in high-density gels that are otherwise too stiff for morphogenesis to occur. Collagen gel contraction and morphogenesis are accompanied by remodeling of collagen fibers around the forming tubules, and this remodeling is likewise regulated by the level of FLNa-β1 integrin interactions. These results support a role for FLNa binding to β1 integrin both as a mechanosensor of matrix tension and as an effector that tunes the balance between matrix stiffness and cellular contraction against that matrix.

The degree by which cells pull on their surroundings is influenced by the stiffness of the matrix through a feedback mechanism (Discher *et al*., 2005; Giannone and Sheetz, 2006). For example, a balance between traction and adhesion forces in response to the stiffness of 3D matrices has been shown to regulate cell migration (Zaman *et al*., 2006). The observation that both decreased and increased FLNa expression disrupts collagen gel contraction and morphogenesis in low-density gels (Figures 2 and 3) suggests that an optimal level of FLNa expression is important during morphogenesis. Interestingly, increasing FLNa binding to β1 integrin, which correlates with enhanced myosin activity, increases matrix contraction and shifts the optimal range for cell morphogenesis to a higher density matrix (Figures 3 and 6). This observation supports the notion that the effects of matrix stiffness can be overcome by enhancing myosin-mediated matrix contraction through FLNa-β1 integrin interactions to tune morphogenesis. A recent study demonstrated a relationship between the biophysical properties of the ECM and myosin activity in regulating branching morphogenesis (Fischer *et al*., 2009). It was demonstrated that endothelial cell branch initiation in a 3D collagen matrix can be inhibited by increased collagen stiffness and myosin activity. However, this study demonstrated that local inhibition of myosin II activity could induce branch initiation in both compliant and stiff collagen gels. Our results imply that epithelial phenotype is regulated by an overall balance of forces outside the cell and those from inside the cell exerted on the surrounding matrix.

Our observations further demonstrate that matrix remodeling through contraction is a key process during epithelial cell morphogenesis. Although gel contraction is a measure to infer contractile activity of cells in the context of global collagen remodeling, SHG imaging is a powerful tool to complement global gel contraction measurements by allowing for the direct observation of structural aspects of type I collagen, such as fibrillar orientation and density, without the need for indirect labeling of collagen using antibodies or fluorescently-tagged proteins (Mohler *et al*., 2003; Provenzano *et al*., 2006). Features of SHG imaging depend on many factors, including the size, density, and orientation of fibrillar collagen (Campagnola and Loew, 2003). Our results suggest manipulation of FLNa binding to β1 integrin affects the local collagen reorganization and fibrillar condensation as indicated by changes in signal intensity adjacent to cell–ECM boundaries. Although matrix remodeling can also include proteolytic degradation, herein we focused specifically on collagen reorganization during cell morphogenesis. It is worth noting that adding a cocktail to inhibit matrix metalloproteinases and other proteases had no effect on collagen fiber remodeling, matrix contraction, nor morphogenesis in either low- or high-density gels (data not shown), demonstrating these processes can occur even in the absence of proteolysis. However, additional studies would be necessary to fully understand the contributions of proteolysis during these collagen matrix remodeling events.

Our findings suggest that culture in a stiff, dense collagen matrix causes an increase in FLNa binding to β1 integrin, although it is not clear how this interaction is regulated. Phosphorylation of FLNa on serine 2152 has been suggested to potentially influence the binding of FLNa to β1 integrin (Vadlamudi *et al*., 2002; Jay *et al*., 2004; Woo *et al*., 2004). However, although FLNa undergoes enhanced phosphorylation in response to force application, the phosphorylation state of serine 2152 does not affect integrin binding to FLNa (19-24), which contains the integrin-binding domain (Glogauer *et al*., 1998; Travis *et al*., 2004). Recently, it was demonstrated that FLNa undergoes intramolecular autoinhibition of integrin binding (Lad *et al*., 2007). Although a mechanism to regulate the autoinhibition of the integrin-binding site of FLNa is not presently known, it is conceivable that mechanical forces acting on filamin, either through

changes in ECM stiffness or internal force generation, might alter the conformation of IgFLNa20, thus releasing its autoinhibitory effect on integrin binding. In support of this, mechanical forces applied through β1 integrins enhance FLNa recruitment to integrin-induced adhesion sites (Glogauer *et al*., 1998; D'Addario *et al*., 2001, 2002). Consistent with this finding, we find that cells cultured in high-density collagen gels undergo enhanced FLNa-β1 integrin interactions (Figure 4).

Although this study demonstrates that FLNa-β1 integrin complexes regulate myosin-mediated gel contraction, the mechanism by which this is accomplished remains a subject for future investigation. One possibility might be that integrin-bound FLNa could enhance the local concentration of cross-linked actin and so increase the number of sites accessible for myosin binding. The amount of actin cross-linking has been shown to be an important determinant of filament contraction and actomyosin ATPase activity (Stendahl and Stossel, 1980; Janson *et al*., 1991). Alternatively, or in addition, FLNa serves as a scaffold for many signaling molecules, including known regulators of myosin-mediated contractility RhoA and Rho-kinase (ROCK) (Ohta *et al*., 1999; Pi *et al*., 2002; Ueda *et al*., 2003), guanine nucleotide exchange factors Trio and Lbc (Bellanger *et al*., 2000; Pi *et al*., 2002), and FilGAP (Ohta *et al*., 2006). Thus, FLNa may alter the signaling that governs myosin-generated contractility. Breast epithelial cell morphogenesis is regulated by RhoA-mediated contractility (Wozniak *et al*., 2003; Paszek *et al*., 2005), and we find that inhibition of the RhoA effector ROCK disrupts collagen gel contraction and branching morphogenesis of hβ1(V787,791I)-expressing cells in high-density gels (data not shown).

We propose that FLNa-β1 integrin is a bidirectional mechanosensitive complex that both regulates collagen matrix contraction during cell morphogenesis in response to changes in collagen density and that it tunes cellular responses to high-density gels through a balance of myosin activity modulated by FLNa-β1 integrin interactions. Although it is likely that multiple proteins are implicated in a mechanosensitive complex, the identification of FLNa-β1 integrin as a component of the complex provides a mechanism that couples the ECM to the cytoskeletal contractile machinery. Furthermore, FLNa signaling through β1 integrin may modulate gel contraction by serving as a scaffold for various signaling molecules. However, further investigation is required to distinguish whether the FLNa-β1 integrin complex serves as a mechanosensor or whether FLNa regulates the β1 integrin mechanosensor complex. Other studies have identified p130Cas and Zyxin as mechanosensitive proteins that undergo changes in conformation and signaling that are implicated in the cellular response to mechanical stretch (Yoshigi *et al*., 2005; Sawada *et al*., 2006). Future work aimed at elucidating how FLNa cooperates with other mechanosensitive proteins will further our understanding of the mechanisms that are involved in matrix contraction and regulation of cell morphogenesis.

These observations may ultimately be of pathological importance, because they may explain some of the underlying mechanisms by which increased mammographic and stromal density might contribute to altered breast epithelial phenotype and breast carcinoma. Breast density is linked to an increased risk of breast carcinoma (Boyd *et al*., 2001) and is associated with a significant increase in the deposition of extracellular matrix components, especially collagen and fibronectin (Guo *et al*., 2001). Furthermore, matrix density could alter treatment efficacy by hindering the delivery of therapeutic macromolecules (Netti *et al*., 2000). Understanding the mechanisms of how environmental factors, such as collagen density, regulate cell phenotype will help elucidate the role of breast density on the development of breast carcinoma.

ACKNOWLEDGMENTS

We thank Drs. Gianluca Gallo, Paul Letourneau, and Suzanne Ponik for critically reading the manuscript and Carolyn Pehlke and Dr. Paolo Provenzano for helpful discussion. Also, we are grateful to the University of Wisconsin Paul Carbone Cancer Center Flow Cytometry Facility for assistance in cell sorting and flow cytometry. This work was supported by National Institutes of Health and National Institute on Aging grant T32 AG-20013 (Sanjay Asthana, principal Investigator; to S. G.), National Institutes of Health National Cancer Institute grant R01 CA-076537 (to P.J.K.), National Institutes of Health National Institute of Biomedical Imaging and Bioengineering grant R01 EB-000184 (to K.W.E.), National Institutes of Health grant R01 GM-068600 (to D.A.C.), and American Cancer Society grant RSG-00-339-04 (to P.J.K.).

REFERENCES

Adelstein, R. S., and Eisenberg, E. (1980). Regulation and kinetics of the actin-myosin-ATP interaction. Annu. Rev. Biochem. *49*, 921–956.

Alexander, N. R., Branch, K. M., Parekh, A., Clark, E. S., Iwueke, I. C., Guelcher, S. A., and Weaver, A. M. (2008). Extracellular matrix rigidity promotes invadopodia activity. Curr. Biol. *18*, 1295–1299.

Bellanger, J.-M., Astier, C., Sarde, C., Ohta, Y., Stossel, T. P., and Debant, A. (2000). The Rac1- and RhoG-specific GEF domain of Trio targets filamin to remodel cytoskeletal actin. Nat. Cell Biol. *2*, 888–892.

Boyd, N. F., Martin, L. J., Stone, J., Greenberg, C., Minkin, S., and Yaffe, M. J. (2001). Mammographic densities as a marker of human breast cancer risk and their use in chemoprevention. Curr. Oncol. Rep. *3*, 314–321.

Brown, E., McKee, T., diTomaso, E., Pluen, A., Seed, B., Boucher, Y., and Jain, R. K. (2003). Dynamic imaging of collagen and its modulation in tumors in vivo using second-harmonic generation. Nat. Med. *9*, 796–800.

Calderwood, D. A., Huttenlocher, A., Kiosses, W. B., Rose, D. M., Woodside, D. G., Schwartz, M. A., and Ginsberg, M. H. (2001). Increased filamin binding to â-integrin cytoplasmic domains inhibits cell migration. Nat. Cell Biol. *3*, 1060–1068.

Campagnola, P. J., and Loew, L. M. (2003). Second-harmonic imaging microscopy for visualizing biomolecular arrays in cells, tissues and organisms. Nat. Biotechnol. *21*, 1356–1360.

Chen, J., Diacovo, T. G., Grenache, D. G., Santoro, S. A., and Zutter, M. M. (2002). The alpha(2) integrin subunit-deficient mouse: a multifaceted phenotype including defects of branching morphogenesis and hemostasis. Am. J. Pathol. *161*, 337–344.

Choquet, D., Felsenfeld, D. P., and Sheetz, M. P. (1997). Extracellular matrix rigidity causes strengthening of integrin-cytoskeleton linkages. Cell *88*, 39–48.

Chrzanowska-Wodnicka, M., and Burridge, K. (1996). Rho-stimulated contractility drives the formation of stress fibers and focal adhesions. J. Cell Biol. *133*, 1403–1415.

Clark, K., Langeslag, M., Figdor, C. G., and van Leeuwen, F. N. (2007). Myosin II and mechanotransduction: a balancing act. Trends Cell Biol. *17*, 178–186.

D'Addario, M., Arora, P. D., Ellen, R. P., and McCulloch, C. A. (2002). Interaction of p38 and Sp1 in a mechanical force-induced, beta 1 integrin-mediated transcriptional circuit that regulates the actin-binding protein filamin-A. J. Biol. Chem. *277*, 47541–47550.

D'Addario, M., Arora, P. D., Fan, J., Ganss, B., Ellen, R. P., and McCulloch, C. A. (2001). Cytoprotection against mechanical forces delivered through beta 1 integrins requires induction of filamin A. J. Biol. Chem. *276*, 31969–31977.

Denk, W., Strickler, J. H., and Webb, W. W. (1990). Two-photon laser scanning fluorescence microscopy. Science *248*, 73–76.

DiDonna, B. A., and Levine, A. J. (2006). Filamin cross-linked semiflexible networks: fragility under strain. Phys. Rev. Lett. *97*, 068104.

Discher, D. E., Janmey, P., and Wang, Y. L. (2005). Tissue cells feel and respond to the stiffness of their substrate. Science *310*, 1139–1143.

Engler, A. J., Sen, S., Sweeney, H. L., and Discher, D. E. (2006). Matrix elasticity directs stem cell lineage specification. Cell *126*, 677–689.

Fischer, R. S., Gardel, M., Ma, X., Adelstein, R. S., and Waterman, C. M. (2009). Local cortical tension by myosin II guides 3D endothelial cell branching. Curr. Biol. *19*, 260–265.

Gardel, M. L., Nakamura, F., Hartwig, J. H., Crocker, J. C., Stossel, T. P., and Weitz, D. A. (2006). Prestressed F-actin networks cross-linked by hinged filamins replicate mechanical properties of cells. Proc. Natl. Acad. Sci. USA *103*, 1762–1767.

Giannone, G., and Sheetz, M. P. (2006). Substrate rigidity and force define form through tyrosine phosphatase and kinase pathways. Trends Cell Biol. *16*, 213–223.

Glogauer, M., Arora, P., Chou, D., Janmey, P. A., Downey, G. P., and McCulloch, C.A.G. (1998). The role of actin-binding protein 280 in integrin-dependent mechanoprotection. The J. Biol. Chem. *273*, 1689–1698.

Guo, W. H., Frey, M. T., Burnham, N. A., and Wang, Y. L. (2006). Substrate rigidity regulates the formation and maintenance of tissues. Biophys. J. *90*, 2213–2220.

Guo, Y. P., Martin, L. J., Hanna, W., Banerjee, D., Miller, N., Fishell, E., Khokha, R., and Boyd, N. F. (2001). Growth factors and stromal matrix proteins associated with mammographic densities. Cancer Epidemiol. Biomarkers Prev. *10*, 243–248.

Ikebe, M., Hartshorne, D. J., and Elzinga, M. (1986). Identification, phosphorylation, and dephosphorylation of a second site for myosin light chain kinase on the 20,000-dalton light chain of smooth muscle myosin. J. Biol. Chem. *261*, 36–39.

Janson, L. W., Kolega, J., and Taylor, D. L. (1991). Modulation of contraction by gelation/solation in a reconstituted motile model. J. Cell Biol. *114*, 1005–1015.

Jay, D., Garcia, E. J., and de la Luz Ibarra, M. (2004). In situ determination of a PKA phosphorylation site in the C-terminal region of filamin. Mol. Cell Biochem. *260*, 49–53.

Keely, P. J., Conklin, M. W., Gehler, S., Ponik, S. M., and Provenzano, P. P. (2007). Investigating integrin regulation and signaling events in three-dimensional systems. Methods Enzymol. *426*, 27–45.

Keely, P. J., Fong, A. M., Zutter, M. M., and Santoro, S. A. (1995). Alteration of collagen-dependent adhesion, motility, and morphogenesis by the expression of antisense alpha 2 integrin mRNA in mammary cells. J. Cell Sci. *108*, 595–607.

Kiema, T., Lad, Y., Jiang, P., Oxley, C. L., Baldassarre, M., Wegener, K. L., Campbell, I. D., Ylanne, J., and Calderwood, D. A. (2006). The molecular basis of filamin binding to integrins and competition with talin. Mol. Cell *21*, 337–347.

Lad, Y., Kiema, T., Jiang, P., Pentikainen, O. T., Coles, C. H., Campbell, I. D., Calderwood, D. A., and Ylanne, J. (2007). Structure of three tandem filamin domains reveals auto-inhibition of ligand binding. EMBO J. *26*, 3993–4004

Larsen, M., Artym, V. V., Green, J. A., and Yamada, K. M. (2006). The matrix reorganized: extracellular matrix remodeling and integrin signaling. Curr. Opin. Cell Biol. *18*, 463–471.

Loo, D. T., Kanner, S. B., and Aruffo, A. (1998). Filamin binds to the cytoplasmic domain of the â$_1$-integrin. J. Biol. Chem. *273*, 23304–23312.

Meshel, A. S., Wei, Q., Adelstein, R. S., and Sheetz, M. P. (2005). Basic mechanisms of three-dimensional collagen fibre transport by fibroblasts. Nat. Cell Biol. *7*, 157–164.

Miron-Mendoza, M., Seemann, J., and Grinnell, F. (2008). Collagen fibril flow and tissue translocation coupled to fibroblast migration in 3D collagen matrices. Mol. Biol. Cell *19*, 2051–2058.

Mohler, W., Millard, A. C., and Campagnola, P. J. (2003). Second harmonic generation imaging of endogenous structural proteins. Methods *29*, 97–109.

Nagano, T., Morikubo, S., and Sato, M. (2004). Filamin A and FILIP (filamin A-interacting protein) regulate cell polarity and motility in neocortical subventricular and intermediate zones during radial migration. J. Neurosci. *24*, 9648–9657.

Nagano, T., Yoneda, T., Hatanaka, Y., Kubota, C., Murakami, F., and Sato, M. (2002). Filamin A-interacting protein (FILIP) regulates cortical cell migration out of the ventricular zone. Nat. Cell Biol. *4*, 495–501.

Naylor, M. J., *et al*. (2005). Ablation of beta1 integrin in mammary epithelium reveals a key role for integrin in glandular morphogenesis and differentiation. J. Cell Biol. *171*, 717–728.

Netti, P. A., Berk, D. A., Swartz, M. A., Grodzinsky, A. J., and Jain, R. K. (2000). Role of extracellular matrix assembly in interstitial transport in solid tumors. Cancer Res. *60*, 2497–2503.

Ohta, Y., Hartwig, J. H., and Stossel, T. P. (2006). FilGAP, a Rho- and ROCK-regulated GAP for Rac binds filamin A to control actin remodelling. Nat. Cell Biol. *8*, 803–814.

Ohta, Y., Suzuki, N., Nakamura, S., Hartwig, J. H., and Stossel, T. P. (1999). The small GTPase RalA targets filamin to induce filopodia. Proc. Natl. Acad. Sci. USA *96*, 2122–2128.

Paszek, M. J., *et al*. (2005). Tensional homeostasis and the malignant phenotype. Cancer Cell *8*, 241–254.

Pelham, R. J., Jr., and Wang, Y.-L. (1997). Cell locomotion and focal adhesions are regulated by substrate flexibility. Proc. Natl. Acad. Sci. USA *94*, 13661–13665.

Pfaff, M., Liu, S., Erle, D. J., and Ginsberg, M. H. (1998). Integrin beta cytoplasmic domains differentially bind to cytoskeletal proteins. J. Biol. Chem. *273*, 6104–6109.

Pi, M., Spurney, R. F., Tu, Q., Hinson, T., and Quarles, L. D. (2002). Calcium-sensing receptor activation of Rho involves filamin and Rho-guanine nucleotide exchange factor. Endocrinology *143*, 3830–3838.

Provenzano, P. P., Eliceiri, K. W., Campbell, J. M., Inman, D. R., White, J. G., and Keely, P. J. (2006). Collagen reorganization at the tumor-stromal interface facilitates local invasion. BMC Med. *4*, 38.

Roeder, B. A., Kokini, K., Sturgis, J. E., Robinson, J. P., and Voytik-Harbin, S. L. (2002). Tensile mechanical properties of three-dimensional type I collagen extracellular matrices with varied microstructure. J. Biomech. Eng. *124*, 214–222.

Sawada, Y., Tamada, M., Dubin-Thaler, B. J., Cherniavskaya, O., Sakai, R., Tanaka, S., and Sheetz, M. P. (2006). Force sensing by mechanical extension of the Src family kinase substrate p130Cas. Cell *127*, 1015–1026.

Schiro, J. A., Chan, B. M., Roswit, W. T., Kassner, P. D., Pentland, A. P., Hemler, M. E., Eisen, A. Z., and Kupper, T. S. (1991). Integrin alpha 2 beta 1 (VLA-2) mediates reorganization and contraction of collagen matrices by human cells. Cell *67*, 403–410.

Sellers, J. R., Spudich, J. A., and Sheetz, M. P. (1985). Light chain phosphorylation regulates the movement of smooth muscle myosin on actin filaments. J. Cell Biol. *101*, 1897–1902.

Sosinski, J., Szpacenko, A., and Dabrowska, R. (1984). Potentiation of actomyosin ATPase activity by filamin. FEBS Lett. *178*, 311–314.

Stendahl, O. I., and Stossel, T. P. (1980). Actin-binding protein amplifies actomyosin contraction, and gelsolin confers calcium control on the direction of contraction. Biochem. Biophys. Res. Commun. *92*, 675–681.

Stossel, T. P., Condeelis, J., Cooley, L., Hartwig, J. H., Noegel, A., Schleicher, M., and Shapiro, S. S. (2001). Filamins as integrators of cell mechanics and signalling. Nat. Rev. Mol. Cell Biol. *2*, 138–145.

Tamariz, E., and Grinnell, F. (2002). Modulation of fibroblast morphology and adhesion during collagen matrix remodeling. Mol. Biol. Cell *13*, 3915–3929.

Tanaka, T., Sobue, K., Owada, M. K., and Hakura, A. (1985). Linear relationship between diphosphorylation of 20 kDa light chain of gizzard myosin and the actin-activated myosin ATPase activity. Biochem. Biophys. Res. Commun. *131*, 987–993.

Travis, M. A., van der Flier, A., Kammerer, R. A., Mould, A. P., Sonnenberg, A., and Humphries, M. J. (2004). Interaction of filamin A with the integrin beta 7 cytoplasmic domain: role of alternative splicing and phosphorylation. FEBS Lett. *569*, 185–190.

Ueda, K., Ohta, Y., and Hosoya, H. (2003). The carboxy-terminal pleckstrin homology domain of ROCK interacts with filamin-A. Biochem. Biophys. Res. Commun. *301*, 886–890.

Umemoto, S., Bengur, A. R., and Sellers, J. R. (1989). Effect of multiple phosphorylations of smooth muscle and cytoplasmic myosins on movement in an in vitro motility assay. J. Biol. Chem. *264*, 1431–1436.

Vadlamudi, R. K., Li, F., Adam, L., Nguyen, D., Ohta, Y., Stossel, T. P., and Kumar, R. (2002). Filamin is essential in actin cytoskeletal assembly mediated by p21-activated kinase 1. Nat. Cell Biol. *4*, 681–690.

Weaver, V. M., Petersen, O. W., Wang, F., Larabell, C. A., Briand, P., Damsky, C., and Bissell, M. J. (1997). Reversion of the malignant phenotype of human breast cells in three-dimensional culture and in vivo by integrin blocking antibodies. J. Cell Biol. *137*, 231–245.

White, D. E., Kurpios, N. A., Zuo, D., Hassell, J. A., Blaess, S., Mueller, U., and Muller, W. J. (2004). Targeted disruption of beta1-integrin in a transgenic mouse model of human breast cancer reveals an essential role in mammary tumor induction. Cancer Cell *6*, 159–170.

Wokosin, D. L., Squirrel, J. M., Eliceiri, K. W., and White, J. G. (2003). Optical workstation with concurrent, independent multiphoton imaging and experimental laser microbeam capabilities. Rev. Sci. Instrum. *74*, 193–201.

Woo, M. S., Ohta, Y., Rabinovitz, I., Stossel, T. P., and Blenis, J. (2004). Ribosomal S6 kinase (RSK) regulates phosphorylation of filamin A on an important regulatory site. Mol. Cell Biol. *24*, 3025–3035.

Wozniak, M. A., Desai, R., Solski, P. A., Der, C. J., and Keely, P. J. (2003). ROCK-generated contractility regulates breast epithelial cell differentiation in

response to the physical properties of a three-dimensional collagen matrix. J. Cell Biol. *163*, 583–595.

Yamato, M., Adachi, E., Yamamoto, K., and Hayashi, T. (1995). Condensation of collagen fibrils to the direct vicinity of fibroblasts as a cause of gel contraction. J. Biochem. *117*, 940–946.

Yoshigi, M., Hoffman, L. M., Jensen, C. C., Yost, H. J., and Beckerle, M. C. (2005). Mechanical force mobilizes zyxin from focal adhesions to actin filaments and regulates cytoskeletal reinforcement. J. Cell Biol. *171*, 209–215.

Zaman, M. H., Trapani, L. M., Sieminski, A. L., Mackellar, D., Gong, H., Kamm, R. D., Wells, A., Lauffenburger, D. A., and Matsudaira, P. (2006). Migration of tumor cells in 3D matrices is governed by matrix stiffness along with cell-matrix adhesion and proteolysis. Proc. Natl. Acad. Sci. USA *103*, 10889–10894.

Zutter, M., Santoro, S., Staatz, W., and Tsung, Y. (1995). Re-expression of the $\alpha 2\beta 1$ integrin abrogates the malignant phenotype of breast carcinoma cells. Proc. Natl. Acad. Sci. USA *92*, 7411–7415.